

**Ore petrology of the Sadiola Gold Mine, Kéniéba Inlier, Mali**

**Mr. Irvin Matsheka (0610418H)**

**Geology Honours (GEOL 4000)**



Cover Photo: Helicopter Pit located at the southern end of the main Sadiola pit. View is north.

**Supervisor: Prof Kim A.A. Hein**

**Chamber of Mines Chair and Professor of Mining Geology**

**University of the Witwatersrand (Johannesburg)**

**School of Geosciences**

## **Table of contents**

<b>List of Figures.....</b>	<b>iii</b>
<b>Declaration .....</b>	<b>iv</b>
<b>Acknowledgements.....</b>	<b>v</b>
<b>Abstract .....</b>	<b>vi</b>
<b>CHAPTER 1: Introduction.....</b>	<b>7</b>
1.1    Preamble.....	7
1.2 Location and Physiography.....	7
1.3 Aims and Objectives.....	8
Figure 1: Locality map of Mali .....	8
<b>CHAPTER 2: Methodology .....</b>	<b>9</b>
Data Collection .....	9
<b>CHAPTER 3: Regional Geology .....</b>	<b>10</b>
3.1 The geology of the West African Craton and the Kedougou-Kéniéba Inlier.....	10
Fig. 2: Simplified geological map of the West African Craton.....	12
Fig. 3: A simplified geological map of the Kedougou-Kéniéba Inlier showing the location of the study area .....	13
3.2 The Geology of the Sadiola opencast mine and the Sadiola deposit .....	14
3.3 Metamorphism .....	15
3.4 Gold Mineralisation.....	15
<b>Chapter 4: Results.....</b>	<b>16</b>
4.1 Drill core results .....	16
4.2 Lithologies .....	19

4.3 Structure.....	21
4.4 Petrography .....	24
4.5 Ore Petrography .....	27
<b>CHAPTER 5: DISCUSSION .....</b>	<b>29</b>
5.1 Depositional Environment .....	29
5.2 Structural Interpretation .....	30
5.3 Petrographic Interpretation.....	30
5.4 Comparison to Sadiola goldfield with the rest of the West African Gold deposits.....	32
<b>CHAPTER 6: CONCLUSION.....</b>	<b>33</b>
<b>Appendix.....</b>	<b>39</b>
<b>Ore petrography.....</b>	<b>42</b>
<b>Core Logging Results .....</b>	<b>43</b>

## **List of Figures**

Figure 1: Locality map of Mali .....	8
Fig. 2: Simplified geological map of the West African Craton (Dioh et al., 2006) .....	12
Fig. 3: A simplified geological map of the Kedougou-Kéniéba Inlier .....	13
Fig. 4: Photographs of the drill core samples.....	18
Fig. 5 : Metasediments of the Helicopter Pit.....	20
Fig. 6: Equal area stereographic projection of bedding .....	21
Fig. 7 : Equal area stereographic projections of cleavage from Helicopter Pit.....	22
Fig. 8: Rose diagrams for the A: Helicopter Pit and the B: Main Pit quartz veins.....	23
Fig. 9: Photomicrograph of SD22-SD37B (Marble) .....	25
Fig. 10: Photomicrograph of SD782-SD29 .....	25
Fig. 11: Photomicrographs of D: SD129-SD77 .....	26
Fig. 12: Photomicrograph of Sample SD129-SD66 .....	27
Fig. 13: Photomicrograph of Sample SD SD782-SD17A .....	28
Fig. 14: Photomicrograph of Sample SD129-SD71.....	28

**Declaration**

I declare that this dissertation/thesis is my own work. I have correctly acknowledged all the sources, to ideas used in this dissertation/thesis. This thesis/dissertation is submitted for a Bachelor of Science degree with Honours in Geology at the University of the Witwatersrand, Johannesburg. It has not been submitted before in any other university for any examination or degree.

Signature: \_\_\_\_\_

Date: \_\_\_\_\_

## **Acknowledgements**

The following project was sponsored by AngloGold Ashanti, Société d'Exploitation des Mines d'Or de Sadiola S.A (SEMODS) and the University of the Witwatersrand. I would like to thank AngloGold Ashanti for providing medical vaccinations, air tickets, accommodation and all the other expenses covered during the field work.

A warm thank you to the Staff at Sadiola Gold Mine for welcoming us and helping where possible. Thank you to the following people for the assistance during the year:

Prof Kim A.A. Hein for being a good supervisor. Thank you very much for your assistance every time I needed it, the constructive comments that made me question a few things. Most importantly thank you for your patience.

The whole West Africa team at the University of the Witwatersrand under the leadership of Prof. Hein

Mr Asinne Tshibubudze (Wits University)

Mr Mamadou Diarra (Sadiola)

Miss Moshala Matabane (AngloGold Ashanti)

Miss Bontle Nkuna (Wits University)

Mr. Musa Manzi

Thanks to my family, and friends. Financial support for the University residences and tuition fees were kindly assisted by Royal Bafokeng Holdings, Steve Kearney Trust.

## **Abstract**

Recent studies on the Sadiola open cast have indicated different metallogenetic styles for the Sadiola gold deposit. The Sadiola open cast occurs with the FE3 and FE4 open cast within the Palaeoproterozoic Kedougou-Kéniêba Inlier of the West African Craton. The Inlier consists of Birimian metasediments which were metamorphosed and deformed during the 2.1 – 1.9 Ga Eburnean orogeny. Metamorphism reached lower greenschist facies as indicated by the chlorite-biotite-cordierite-calcite-dolomite mineral assemblages. The Sadiola deposit is hosted by the Kofi Formation which is currently undated. The Kofi Formation is made up of Birimian-type sediments and they include greywacke, shale and graphitic shale with conglomeratic interbeds, banded iron formations and carbonates.

The alteration types recorded in the host rocks are potassic, silicification, dolomitisation, chlorite-biotite alteration, calc-silicate and sulphidation. The common sulphide minerals are pyrite, arsenopyrite and pyrrhotite with minor magnetite and sphalerite. The following paragenetic sequence is observed for the ore mineralogy: pyrite – chalcopyrite - ( $\pm$  sphalerite) – arsenopyrite. Gold is paragenetically associated with pyrite and arsenopyrite. The rocks also show evidence of deformation through kinked biotite and the development of stylolites. Two metamorphic events are recorded at Sadiola: regional metamorphism to greenschist facies and contact metamorphism to hornblende-hornfels facies.

Sadiola deposit is therefore classified as either an intrusion-related gold deposit or a thermal aureole gold deposit, which are all subclasses of orogenic gold deposits. Mineralisation at the Sadiola deposit is spatially and temporally associated with the tonalite-granodiorite plutons and tonalite dykes. The Sadiola Fracture Zone served as the fluid conduit and mineralisation occurs along the inner to middle contact aureole. The ubiquitous occurrence of biotite marker in polished thin sections is interpreted as indicating biotite isograd and marks the division between rocks that have been completely recrystallised at Sadiola to rocks in which the primary bedding is still preserved.

## **CHAPTER 1: Introduction**

### **1.1 Preamble**

The giant Sadiola opencast gold mine is located within the Sadiola goldfield in Mali in the Kedougou-Kéniéba Inlier (KKI), which is part of the West African Craton (WAC). The goldfield also hosts the FE3 and the FE4 open casts. These together with the Sadiola opencast mine are mined by Société d'Exploitation des Mines d'Or de Sadiola S.A (SEMOS), which is a joint venture between the government of Mali, IAMGOLD, IFC and AngloGold Ashanti. Mining in the Sadiola opencast commenced in 1996 and the opencast is currently reviewing its resources and reserves.

This research project concentrates primarily on the ore genesis of the Sadiola gold mine. Various deposit styles have been suggested for the Sadiola deposit in the sub-classes of an orogenic type deposit (Goldfarb et al., 2001). Mineralisation at Sadiola has been shown to have a temporal and a spatial relationship to the tonalite-granodiorite plutons and tonalite dykes. Sadiola is located in close proximity to the Alamoutala-Sekokoto-Kakadian plutonic system. Mineralisation has shown to be as a result of the fluids and metamorphism associated with the intrusions (Hein and Tshibubudze, 2007b). Determining the paragenesis, investigation of the mineralogical, microstructural and alteration events will assist in determining gold mineralisation, and is considered important for the Sadiola exploration and in-mine development.

### **1.2 Location and Physiography**

The Sadiola opencast mine is located within the Sadiola village. The village is situated in the south-western part of Mali at about 77km south of the regional capital, Kayes (Fig. 1) near the border of Mali and Senegal. Mali is a semitropical to arid landlocked country which is part of the West African Savannah-Sahel region (Fig. 1). It extends over 1, 240, 278 square kilometres in size. Its estimated population was recorded at 12.5 million as at 2006 with an annual growth rate of 2.4%. French serves as an official language with 80% of the population speaking Bambara. The main religion is Muslim, with Christian and other religions estimated at 10% of the population.

In 2006, the country's GDP was estimated at \$5.847 billion with an annual growth rate estimated at 5.1%. The country's GDP puts Mali as one of the poorest countries in the world. The main sectors that contribute largely to this GDP are mining, agriculture and livestock farming and Mali is currently the 3<sup>rd</sup> largest producer of gold in the continent after the Republic of South Africa and Ghana. Mining is a growing industry in the country and gold mining accounts for approximately 80% of the mining activity. Gold became the number one mining export in Mali with AngloGold Ashanti and Randgold being two of the biggest mining houses in the country (US Department of States).

### 1.3 Aims and Objectives

The main aim of this project is to define the Sadiola deposit style with a particular interest in the petrology, paragenesis, structure, mineralogy of the deposit and its genetic model. This will then be used to compare the model with other gold deposits in the WAC. The key features that will help in classification include describing and characterising the mineralogical textures and their significance to ore forming processes, the alteration systems and the mineral association.



Figure 1: Locality map of Mali (US Department of States).

## **CHAPTER 2: Methodology**

### Data Collection

This research comprised two important tasks: petrographical work and field work which were preceded by literature review. Field work was completed in June 2009 and involved examining drill-core and mapping of the host rocks. Six drill cores from the Sadiola Deep Sulphide project were examined and these include SD022, SD042, SD048, SD119, SD129 and SD782. Samples were collected in 2008 and polished thin sections were prepared by SGS Laboratories in Booysens, Johannesburg.

Field mapping involved mapping of the West High-Wall of the main pit and the Helicopter pit at the southern end of the main Sadiola pit. At each station point the following (if present) were recorded: lithology, bedding and cleavage orientation, faulting, folding, alteration and the distance from the station point to the face wall. Station points were distanced at 10R intervals at which R is the approximated to be 1.02m. Stratigraphic facing was determined based on sedimentary features i.e. cross-bedding or turbidites. The measured orientations (strike/dip/dip direction) were plotted on equal area stereonet projection using the GeOrient© 9.4.0 software.

Six diamond drill cores were examined based on the lithological contacts. From this, the depth of the drill core was recorded, as well as alteration and mineralogy. The hole size, azimuth and dip was recorded. Pits maps were provided by SEMOS on site.

A petrographic study was completed at University of the Witwatersrand. For each thin section, mineral assemblage, mineral textures, cross-cutting relationship and sulphide mineralogy were recorded.

## **CHAPTER 3: Regional Geology**

### **3.1 The geology of the West African Craton and the Kedougou-Kéniéba Inlier**

The West African Craton (Fig. 2) is a piece of continental crust that has been stable since approximately 1.7Ga (Dia et al., 1997). It is divided into the Man shield in the south and the Reguibat shield in the north. The two shields are separated by the upper Proterozoic to Paleozoic sedimentary Taoudeni basin. The Reguibat Rise and the Man terrains are composed of Archaean to Proterozoic rock formations (Potrel et al., 1998) with the Palaeoproterozoic rocks of the Man shield referred to as the Birimian sequence (Beziat et al., 2000).

The Kéniéba and Kayes inliers are situated towards the western border of Senegal and Mali (Fig. 2). The WAC crops out in western Mali in what is known as the Kedougou-Kéniéba Inlier (Dia et al., 1997). The Birimian sequence represents a large sedimentary basin and a volcanic belt which correlates well with the 2.1 Ga accretion period during the Eburnean orogeny (Milesi, 1992). The Palaeoproterozoic Biriman Kedougou-Kéniéba Inlier (KKI) in the West African Craton can be divided into three distinct domains: the eastern, central and the western domain (Matabane and Hein, submitted). The central and eastern domains are separated by the Senegalo-Malian Shear Zone (SMF) while the central and western domains are separated by the Main Transcurrent Shear Zone (MTZ) (Fig. 3).

The geology of these domains is defined largely by Boshoff et al. (1989), Ledru et al. (1991), Wilson, (2002), Dioh et al. (2006) and Gueye et al. (2008):

\* The western domain is composed of the Mako Supergroup, which is a volcanic sequence that consists of tholeiitic basalt and andesite. It also consists of tholeiitic pillow basalts. The pillow basalts have an NMORB affinity, while the massive basalt has an enriched MORB composition. It is also characterised by folded low-grade metamorphic rocks which are intruded by granitic and mafic bodies. The Mako Supergroup is intruded by the Sandikounda Layered Complex and the Laminia Kaourou Plutonic Complex (2160-2130 Ma). The NW-SE trending Mako volcanic belt is located west of the Main Transcurrent Zone.

\*The central domain is dominated by the Diale-Dalemé Supergroup which is a sedimentary to volcano-sedimentary unit. It is composed of detrital sedimentary rocks interbedded with calc-alkaline volcanic rocks. The sedimentary rocks are isoclinally folded with the folds being upright and overturned to the SE-direction. It is intruded by the Saraya plutonic complex and the Balangouma and Boboti plutons. The Diale-Dalemé occurs with the Faleme volcanic belt which consists of andesite and felsic lava, with

chemical sediments being observed throughout the belt. The Main Transcurrent Zone follows the lithological contact between the Mako and the Diale-Dalema Supergroups.

\*The eastern domain hosts the Sadiola goldfield in the Kofi Formation (Bishoff et al., 1989; Ranson, 1998; Wilson, 2002). This formation is also referred to as the Dalema-Kofi Supergroup and lies east of the Senegalo-Malian Shear Zone. The Kofi Formation is dominated by metasedimentary rocks (Ranson, 1998; Wilson, 2002). These rocks are classified as Biriman-type sediments and include greywacke, shale and graphitic shale with conglomeratic interbeds, banded iron formations and carbonates (Hanssen et al., 1978).

The Dalema-Kofi Supergroup is crosscut by tourmaline-rich quartz veins which are the primary host to gold mineralisation (Wilson, 2002) in the Loulo goldfield, SSE of Sadiola, near the town of Kéniéba. Ranson (1998) indicated that gold mineralisation occurs in pelitic shales. The Dalema-Kofi sequence is currently not dated (Dioh et al., 2006; Matabane, 2008). It is transacted by the Senegalo-Malian Shear Zone with several gold deposits located in close proximity to the structure (Boshoff et al., 1998).

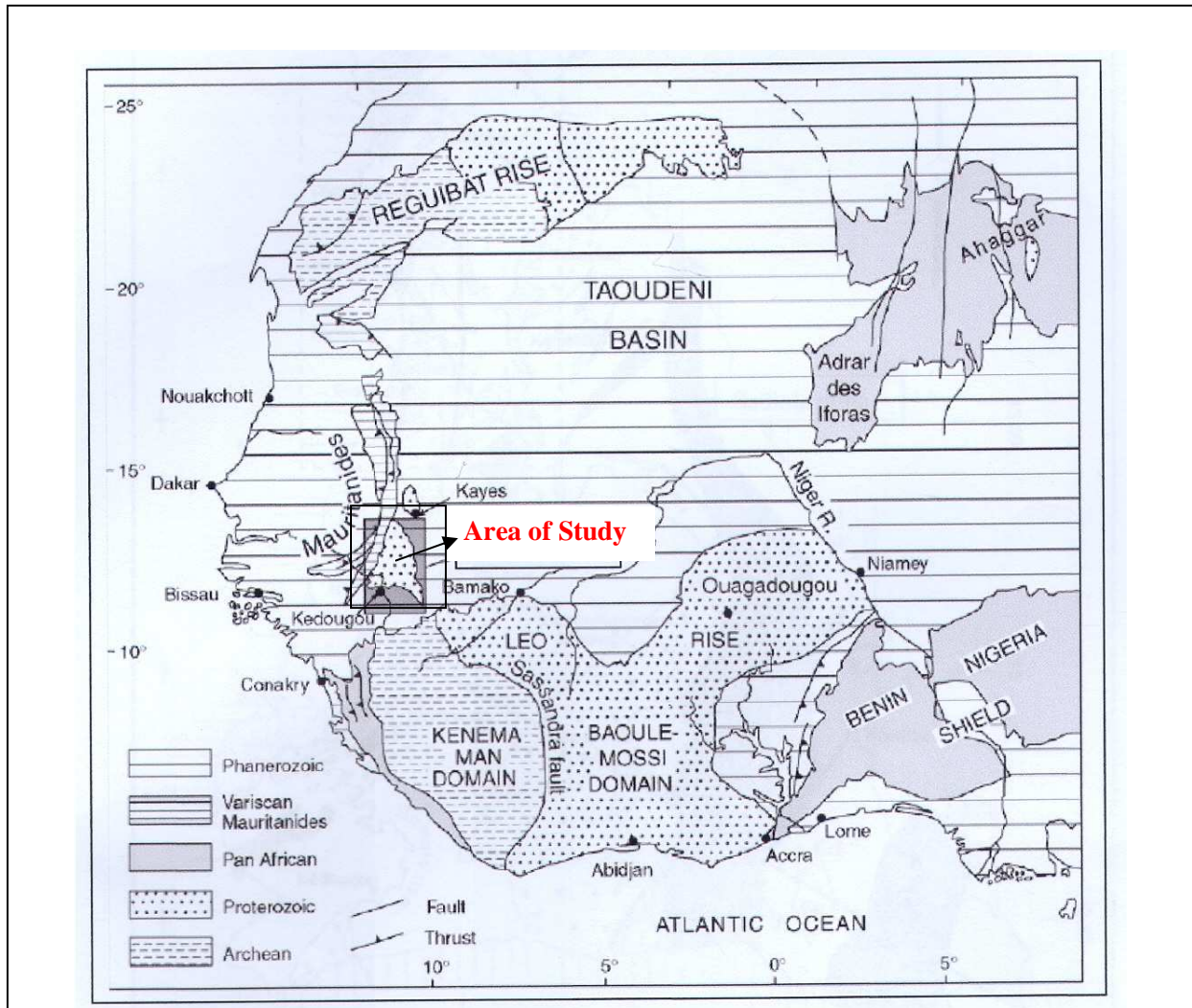


Figure. 2: Simplified geological map of the West African Craton (Dioh et al., 2006).

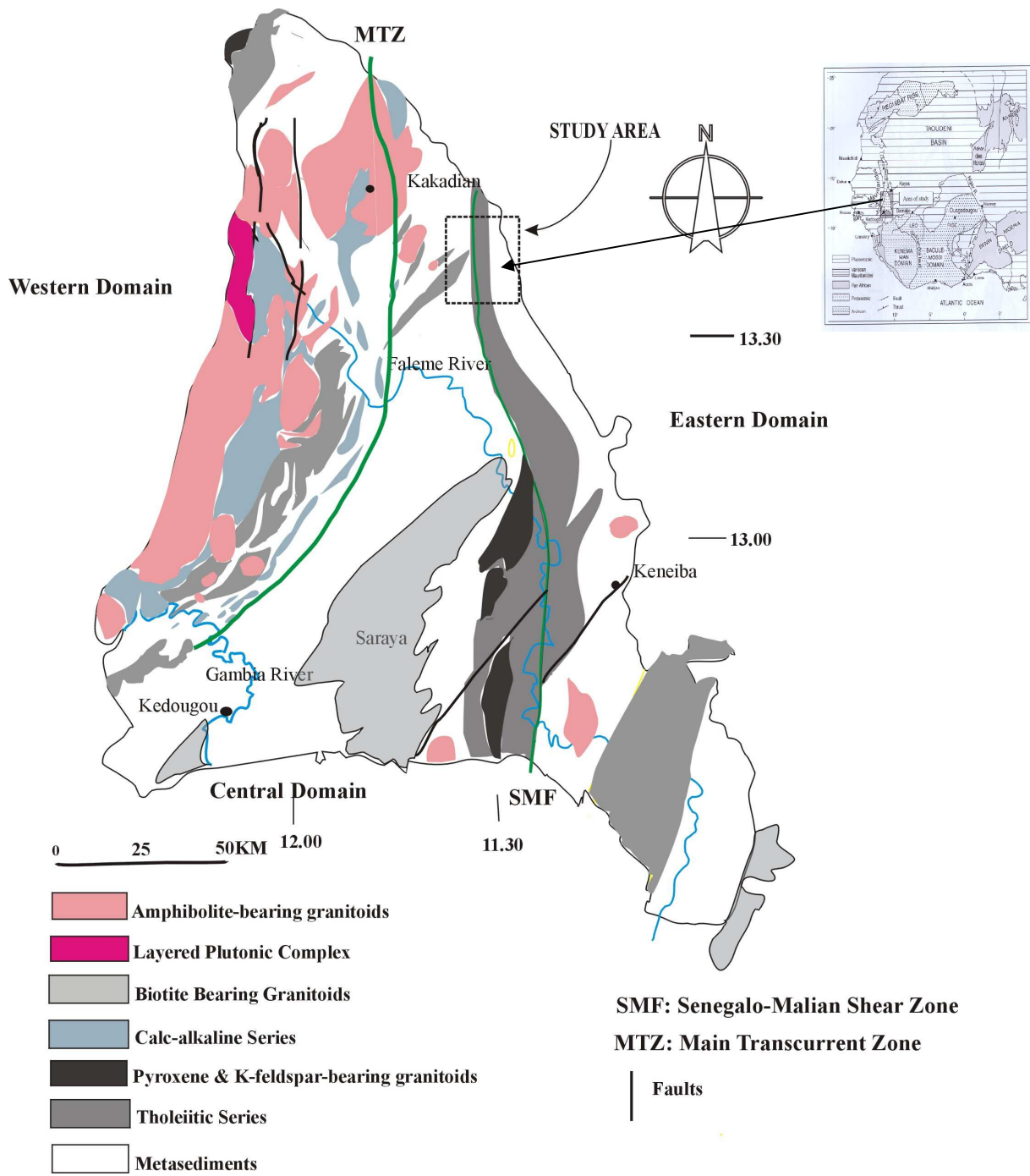


Figure. 3: A simplified geological map of the Kedougou-Kéniéba Inlier showing the location of the study area (redrawn from Dioh et al., 2006).

### 3.2 The Geology of the Sadiola opencast mine and the Sadiola deposit

The Kofi Formation of the Kedougou-Kéniêba Inlier is dominated by fine-grained carbonaceous greywacke, alternating greywacke-shale units, impure carbonates which were folded and contain limestone beds, siltstone, minor tuff and volcanoclastics units (Boshoff et al, 1998; Hanssen et al., 1998; Hein and Tshibubudze, 2007a, b). Jordaan et al. (1994) indicated that calcitic marbles occur in the Kofi Formation. The Sadiola goldfield consists of greywacke, siltstone, marble, carbonaceous to volcanoclastic greywacke and BIF shale (Hein and Tshibubudze, 2007a, b). The goldfield occurs along a marble-greywacke contact located east of the Senegalo-Malian Shear Zone (Hanssen et al., 1998).

The greywacke units of the Sadiola goldfield are best developed to the west of the Sadiola Fracture Zone, while impure carbonates are best developed to the east. The Sadiola Fracture Zone is interpreted to be a splay of the Senegalo-Malian Shear Zone. Carbonate units are the main host to the Sadiola deposit (Boshoff et al., 1998). The lithologies of the Sadiola goldfield show evidence of macroscopic to mesoscopic slump structures (Hein and Tshibubudze, 2007a, b). The slump structures in the Sadiola goldfield were defined by Matabane (2008) in the FE3 open casts, but occur throughout the Sadiola goldfield.

There is however a lack of detailed stratigraphy for the Kofi Formation in the literature. Jordaan et al. (1994) outlined the stratigraphy of the Kofi Formation: the formation is over 500m in thickness and is dominated at the base by arenitic tourmalinite, overlain by green argillite, interbedded pink arenite, calc-silicate, followed by the calcitic marble and pelite, which is locally dolomitised. The sequence is capped by fine-medium grained arenite, siltstone, tourmalinite and intermediate lava. The Sadiola hanging-wall is composed of greywacke (Sheets and Moore, 2000a; Hanssen, 1998; Van der Merwe, 2002; Hein, 2008) to metagreywacke (Sheets and Moore, 2000b). The hanging-wall consists of greywacke unit, carbonate bearing units, fine-grained distal turbidite units, tuffaceous and acid volcanic units (Sheets and Moore, 2000a, b). Sheets and Moore (2000a) used the Sadiola Fracture Zone as the division between the hanging wall and the footwall.

The footwall consists of marble which is interbedded with pelitic beds. Three types of marble are recognised by Hanssen (1998) and include contorted, disrupted and transposed marbles. The carbonate units are massive to bedded texture and they are succeeded by a slump facies (Hein, 2008). Quartz-feldspar porphyry and diorite dykes cross-cuts both the hanging wall and the footwall greywacke and marble units respectively (Moore and Sheets, 2000a, b; Ranson, 1998; Hanssen et al, 1998). The greywacke unit has been cross-cut again by dolomite and quartz veins (Ranson, 1998).

### **3.3 Metamorphism**

Metamorphism associated with the Eburnean orogeny has affected the Birimian sequence (Hastings, 1982). Metamorphic grade is recorded as low-pressure greenschist facies as indicated by the mineral assemblage muscovite, chlorite,  $\pm$  biotite mineral assemblage (Ledru et al., 1991). Liégeois et al., (1991) recognised a mineral assemblage indicative of the biotite-chlorite transition in the greenschist facies. These greenschist minerals are fine-grained and show a granoblastic texture with no indication of porphyroblastic texture. Green to brown biotite and cordierite mineralogy is observed in contact-metamorphic aureoles of the plutons. The carbonates are recrystallised to marbles and the sequence reached hornblende hornfels facies occurs near the contact aureole of the granitoids (Ledru et al., 1991; Hein et al., 2004; Hein, 2009).

Liégeois et al. (1991) concluded that metamorphism was syn-tectonic based on the orientation of sheet silicates and amphiboles. The KKI sediments were then intruded by various granitoid plutons which caused further metamorphism (Dioh et al., 2006). The four types of granitoids that intruded the sediments of the KKI are sodic calc-alkaline granitoids, amphibole bearing granitoids, pyroxene and K-bearing granitoids and the peraluminous biotite bearing units (Dioh et al., 2006). In the Sadiola goldfield, two metamorphic events are recorded: regional metamorphism to greenschist facies and contact metamorphism (Hein and Tshibubudze, 2007a, b). Contact metamorphism is defined as the metamorphism that occurs in close proximity to intrusions and has formed as a result of heat from the intrusion (Blatt et al., 2006). Metamorphism at Sadiola reached hornblende-hornfels facies as a result of the emplacement of tonalite-granodiorite plutons and the tonalite dykes (Hein and Tshibubudze, 2007a, b).

### **3.4 Gold Mineralisation**

Three types of gold mineralisation have been recognised in the West African Craton. These are pre-orogenic, syn-orogenic and late-orogenic mineralisation. Mineralisation is related to regional tectonic event (Milesi et al, 1992; Beziat et al., 2008). Pre-orogenic deposits are associated with early extensional zones and are recorded in stratiform Au tourmalinite in the Loulo goldfield in Mali (Milési et al., 1991; Fouillac et al., 1993; Béziat et al., 2008). Syn-orogenic mineralisation is associated with mineralisation in disseminated sulphides in volcanic and plutonic rock (Milési et al., 1992). Late-orogenic deposits are characterised by disseminated gold-bearing arsenopyrite and Au-quartz lode and quartz-vein type. These are interpreted as the major type and host of gold in West Africa (Milési et al., 1991). Two metallogenic styles have been observed in the Sadiola goldfield by Hein and Tshibubudze (2007a, b) and these are placer gold in the palaeochannels and scree and gold occurring in stockwork veins and breccias.

## **Chapter 4: Results**

### **4.1 Drill core results**

Sample description involved a detailed study of the core samples and describing the rock types, alteration sequence and paragenesis (if possible) of the overall individual core logs. The following table summarises the events from the drill core samples.

Table 1. The paragenetic sequence observed in the samples from the six Borehole cores.

<b>Sequence of Events</b>	<b>SD 129</b>	<b>SD 042</b>	<b>SD 022</b>	<b>SD 119</b>	<b>SD 782</b>	<b>SD 048</b>
1. Deposition of the sediments	x	x	x	x	x	x
2. Slump of sediments	x				x	x
3. Lithification	x	x	x	x	x	x
4. Fracturing and Dilation	x	x	x	x	x	x
5. Vein development	x	x	x	x	x	x
6. Silica rich vein	x	x	x	x (with calcite)	x	x
7. Sulphide rich deposits in the vein	x	x	x	x	x	Epidote
8. Disseminated sulphides	x	x		x	x	Chlorite
9. Later Epidote and chlorite	x		x	x	x	Sulphides

The overall sequence of events includes:

1. (a) Deposition of sediments.  
(b). Slumping of sediments.
2. The sediments were lithified.
3. Fracturing and dilation and formation of open-space fill.
4. Precipitation of disseminated sulphides.
5. The last stage is the development of epidote and chlorite. The chlorite occurs as spots in the matrix.

The observed lithologies in the drill cores are greywacke and marble unit. The major alteration types are calc-silicate, potassic, silicification and sulphidation. The major ore minerals are oxidized pyrite and pyrrhotite. Minor ankerite veins were also recognized in the marble unit. The greywacke and the marble unit are separated by an oxidized carbonaceous-siltstone greywacke. This sequence is also observed in five of the drill cores. The veins that cross-cut the greywacke unit are zoned. These are quartz-calcite-sulphides and pyrite-calcite-quartz zoning. Pyrite also develops as an open space fill. The mineralogy of the greywacke unit showed a randomly oriented mineral texture and with chloritoid spots, euhedral hornblende and biotite in an equiangular texture in borehole SD129. This texture implies that the grains have triple point boundaries and are in textural equilibrium.

The observed sequence in borehole SD782 is an oxide zone from about 93m to 183m that grades into a marble unit. The oxide zone is mainly composed of metasediments, sandy siltstone and a slump sequence. The zone is Fe-altered. Primary bedding has been destroyed in this zone, but is still preserved in the marble unit. Soft sediment deformation structures were observed in the marble unit. Slumping which occurred prior to the lithification processes are the main soft-sediment structures observed.

The carbonaceous-siltstone greywacke unit grade from sulphidated greywacke at the contact with the greywacke unit, to a sulphide rich zone and finally into a sulphidated carbonate at the contact with the marble.

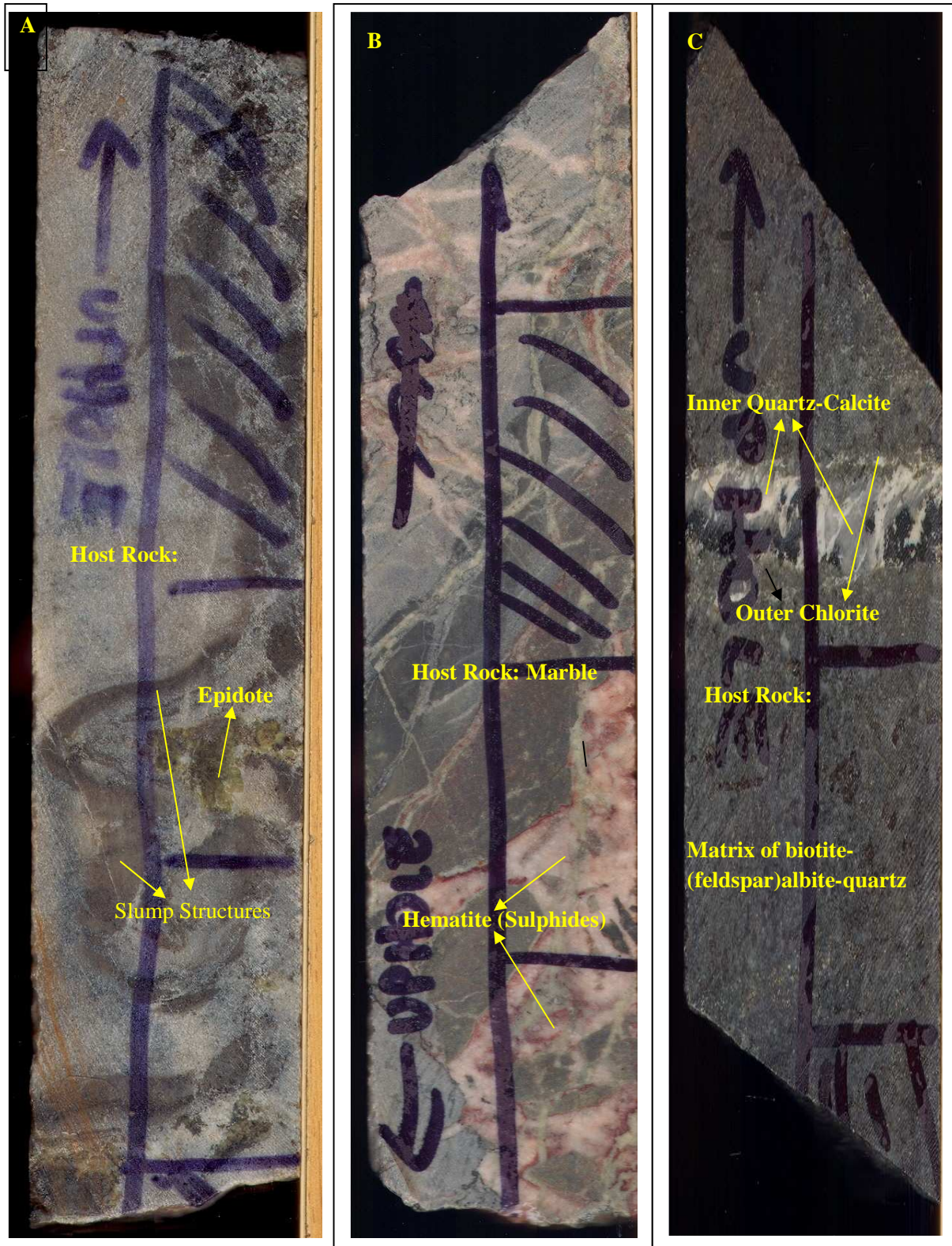


Figure. 4: Photographs of the drill core samples showing some of the observed mineralogy and textures. A: SD22-SD40: Soft Sediment structures and epidote mineralogy observed in the marble unit. B: SD22-SD36: Brecciated marble unit with later sulphide (hematite) and potassic-alteration development. C: SD119-SD59: Greywacke unit with a zoned vein of outer chlorite and inner silica-calcite and sulphide composition. Photos taken by Prof. Hein in 2007.

#### **4.2 Lithologies**

Mapping was undertaken in two areas in the Sadiola open cast: West high-wall in the main pit and the Helicopter pit located at the southern end of the main pit (Map 1 & 2). The main lithologies observed in the main pit are metagreywacke and carbonates. The greywacke sequence is massive in texture and the visible mineralogy includes quartz, calcite, minor sulphide and epidote in some cases. The carbonate sequence becomes friable and less competent at the contact with the carbonaceous-siltstone greywacke unit. This unit is interpreted as the Sadiola Fracture Zone (SFZ) as defined by Hein (2009) and Boshoff et al (1998). Pyrolusite, epidote and kaolinite occur in this zone and the zone is cross-cut by quartz veins. It is heavily oxidized, silicified and kaolinised meaning that the unit is very decomposed.

A carbonate sequence is exposed in the pit face to the east of the Sadiola Fracture Zone. . The mineralogy of the carbonate sequence includes biotite, calcite and sulphide. The sequence is massive at the contact with the SFZ, gradational with a bedded carbonate. Euhedral crystals of hornblende and calcite crystals are set in fine-grained bedded matrix comprising epidote, sulphides, calcite and quartz. This texture is interpreted as a result of skarnification. Further to the east, the exposed carbonate sequence hosts micro-folds. It varies from hornfels-biotite rich marble, epidote-rich marble and calcite-rich marble. An anticline is developed in the carbonate sequence.

Three upper benches were mapped in the Helicopter pit (Map 1). These benches consist of sandy metasediments and are cross bedded. The metasediments include slump sequences with minor seismites. Primary bedding is destroyed in some of the metasediments. The sequence is fine-grained and hosts quartz veins. The helicopter metasediments are folded by a tight anticline with the fold hinge hosting a major fault (Fig. 5).

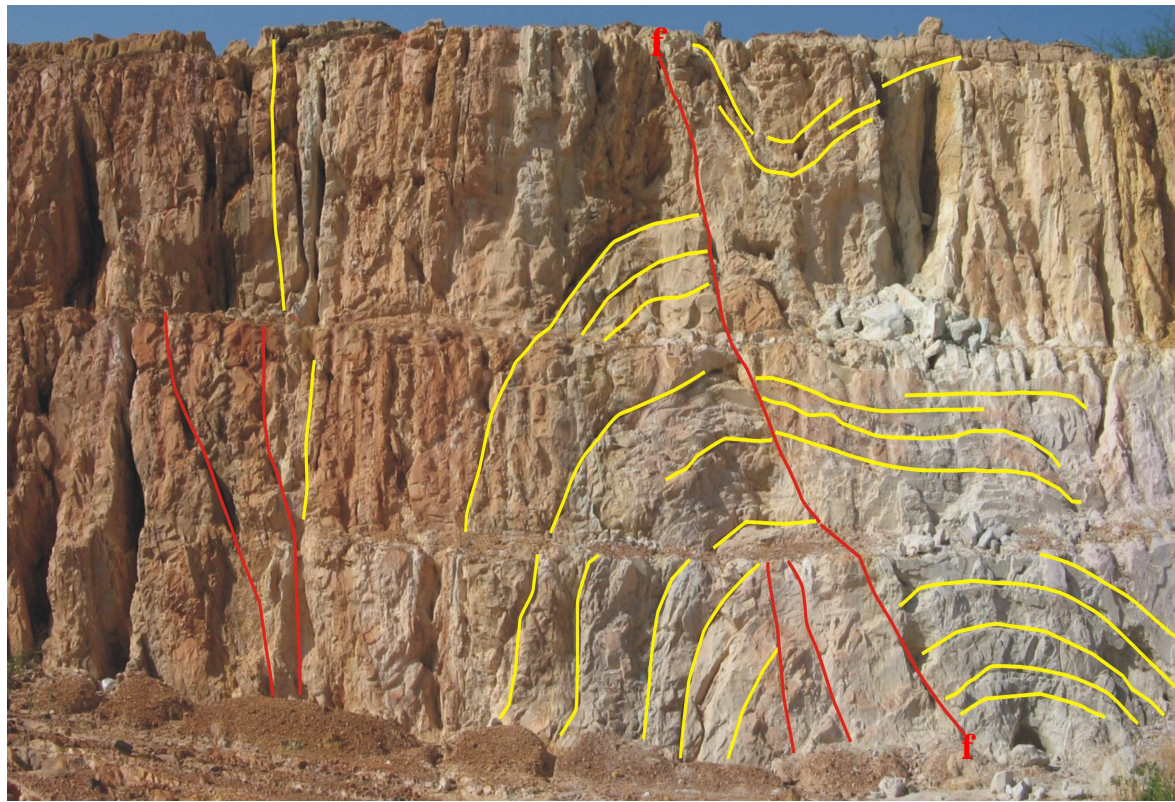


Figure. 5 : Metasediments of the Helicopter Pit. These are folded with a fault at the fold hinge. The fault is oriented at  $010^0/66^0$ /W. Photograph taken from the Helicopter Pit facing south.

#### 4.3 Structure

Two deformation events are recorded for the study areas in the Sadiola deposit. These are interpreted from equal area stereographic projections of bedding and the discontinuous, parallel cleavage in the metasedimentary rocks. The equal area stereographic projections of bedding from the Helicopter Pit records a calculated mean bedding of  $336^{\circ}/64^{\circ}\text{E}$  with a calculated mean for the west high-wall of  $350^{\circ}/51^{\circ}\text{W}$ . The spread of the data around the primitive circles is related to folding about a NNW-trending fold axes (F1) and refolding of F1 about the ENE-ESE trending fold axes (F2). Bedding is rotated against minor faults (Fig. 6).

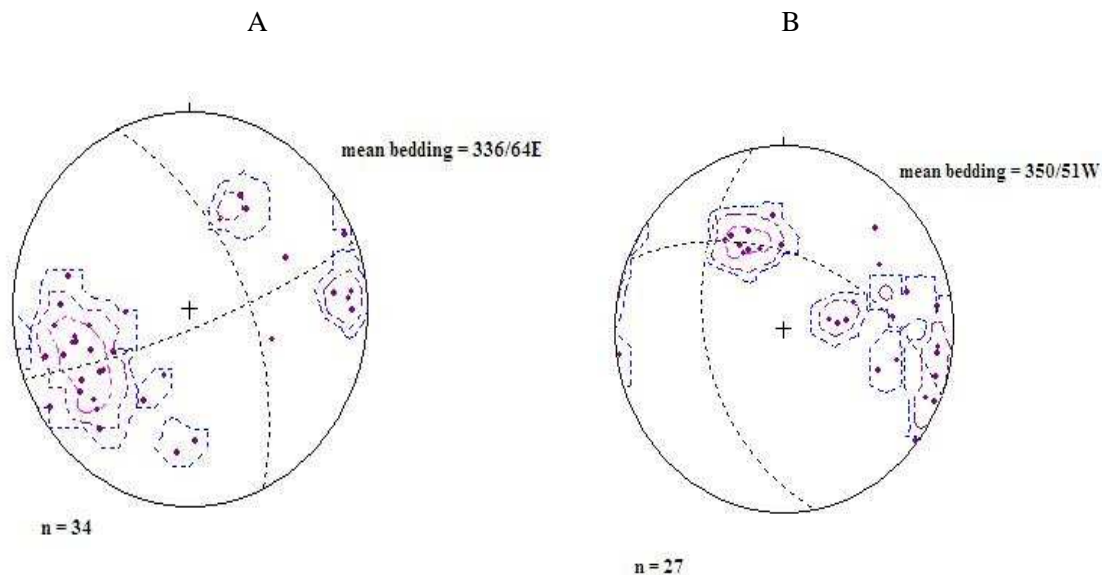


Figure. 6: Equal area stereographic projection of bedding from A: Helicopter Pit & B: West High-wall in the main pit.

The equal area stereographic projections of cleavage of the Helicopter Pit records a calculated mean cleavage of  $343^{\circ}/54^{\circ}\text{E}$ , however the data can be resolved into two data sets: a NNW trending set and a NE-trending set (Fig. 7). Two sets of cleavages were also observed by Hein (2009) in which the ENE trending sets (S2) cross-cuts the NNW-trending sets (S1). Unfortunately this cross-cutting relationship has not been observed in the study area, but is accepted by the mine as a tectonic sequence for the Sadiola pit. The calculated mean for the NNW-trending cleavage is  $332^{\circ}/60^{\circ}\text{E}$ , while the ENE trending cleavage is  $061^{\circ}/43^{\circ}\text{S}$ . The spread of data about the primitive circle for the NNW-trending cleavage is as a result of folding by F2 (Fig. 7).

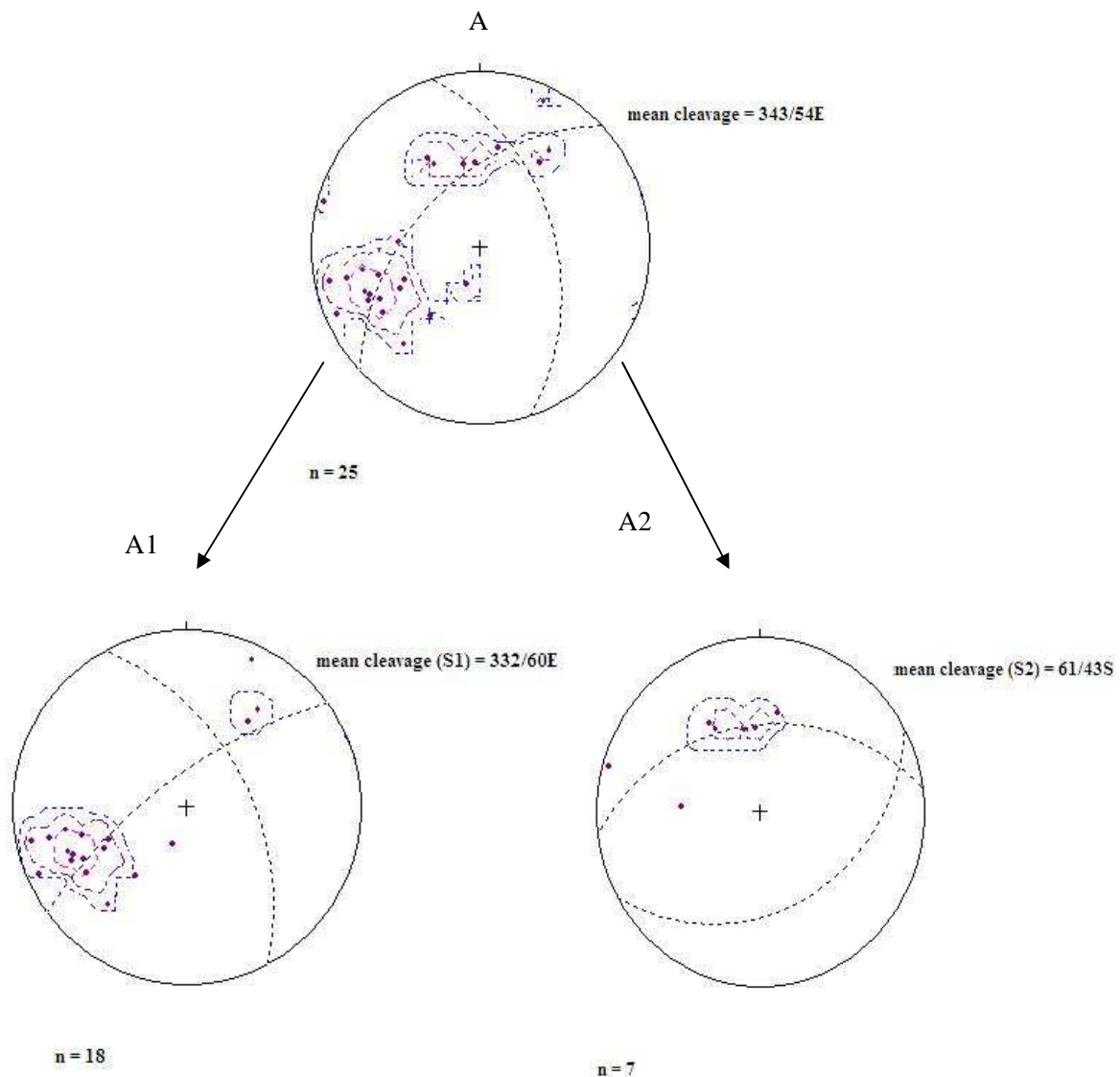


Figure. 7 : Equal area stereographic projections of cleavage from Helicopter Pit. The data is resolved into two data sets : A1= S1 & A2= S2.

Stereographic projections for the cleavage from the west high-wall in the main pit is not presented because only five data points were collected and were therefore considered to be insufficient. However the calculated mean was  $213^{\circ}/72^{\circ}$ E.

Rose diagrams for quartz veins from the Helicopter Pit and the west high-wall are presented in Figure 8. The dominant trend of quartz veins in the Helicopter Pit is NE with sub-ordinate trend towards NNE, while the dominant trend of the quartz veins in the west high-wall is NNE with the sub-ordinate trend towards NNW. The quartz veins elsewhere in the main pit are folded by F2 (Hein, 2009) indicating that the veins formed prior to S2. The relationship between S1 in the Helicopter Pit and the dominant orientation of quartz veins suggest that they formed at the same time during the NE directed compression. This is because bedding and cleavage verge towards NE.

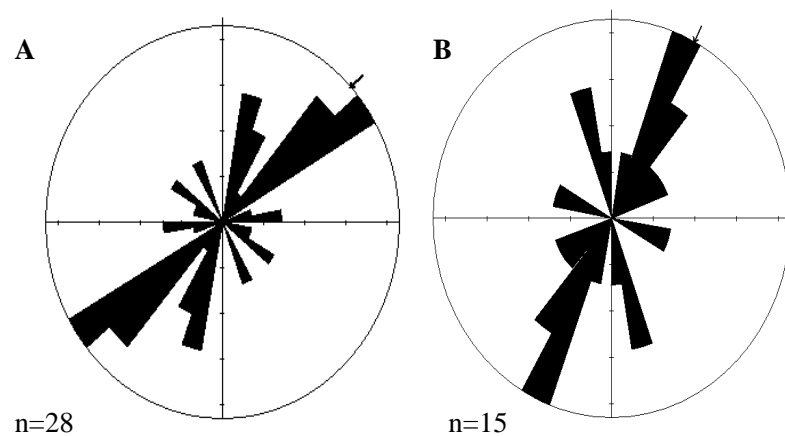


Figure. 8: Rose diagrams for the A: Helicopter Pit and the B: Main Pit quartz veins.

#### **4.4 Petrography**

The lithologies of the Sadiola gold mine vary from bedded/skarnified marble to marble and greywacke. They range from fine-grained to coarse-grained. The boundary between the textures is marked by randomly oriented biotite (Fig. 9) although this texture was not observed in all the samples. The matrix minerals are biotite, calcite, dolomite, quartz and minor feldspar (albite), chloritoid, chlorite, hornblende, cordierite, epidote and tourmaline (Fig. 9, 10, 11). Magnetite is an accessory mineral. Minor cordierite occurs with hornblende in sample SD782-SD16. The dominant alteration types are potassic, chlorite, carbonatization (dolomitisation) and sulphidation. The biotite has been altered to chlorite, and chlorite is also accompanied by potassic alteration. Potassic alteration is shown by the development of the albite and it overprints quartz. The alteration paragenesis sequence is interpreted as: silicification – calc-silicate/propylitic – dolomitisation – potassic alteration & biotite-chlorite – sulphidation. Propylitic alteration is indicated by the occurrence of chlorite, epidote and tremolite. Evidence of deformation is shown by kinked to radiating biotite, stylolites and a triple point grain contact between the dolomite. This is interpreted as a result of pressure solution.

Stylolites were recorded between the calcite. Biotite is generally absent in epidote-rich samples. Chloritoid overgrowths were also recorded with some being zoned and euhedral. The zoned chloritoid consists of an inner semi-rounded crystal. The chloritoid are interpreted to have precipitated late as they cross-cut the quartz-albite-epidote matrix and the coarse calcite veins. Minor muscovite and tremolite were observed in sample SD22-SD51B (meta-greywacke), and are associated with potassic and dolomitisation alteration. Two generations of dolomite have been identified. The early dolomite forms part of the matrix and the later is vein dolomite. Two generations of calcite were also identified: matrix calcite and later coarser calcite in veins. Sulphide mineralogy also occurs in two generations: disseminated and vein sulphides. The following paragenesis was observed for the Sadiola mineralogy: quartz – calcite – dolomite - biotite – sulphides – dolomite with sulphides-quartz-calcite vein – chloritoid.

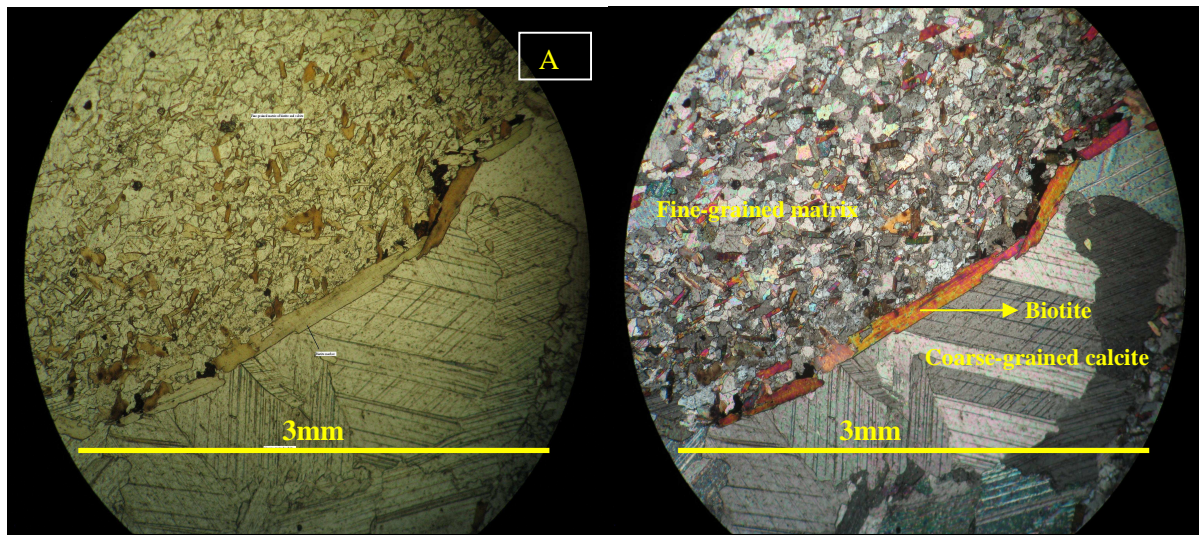


Figure. 9: Photomicrograph of biotite separating the fine-grained matrix of biotite-calcite and the coarse-grained calcite from sample SD22-SD37B (Marble). There is no observed biotite mineralogy in the coarse-grained calcite.

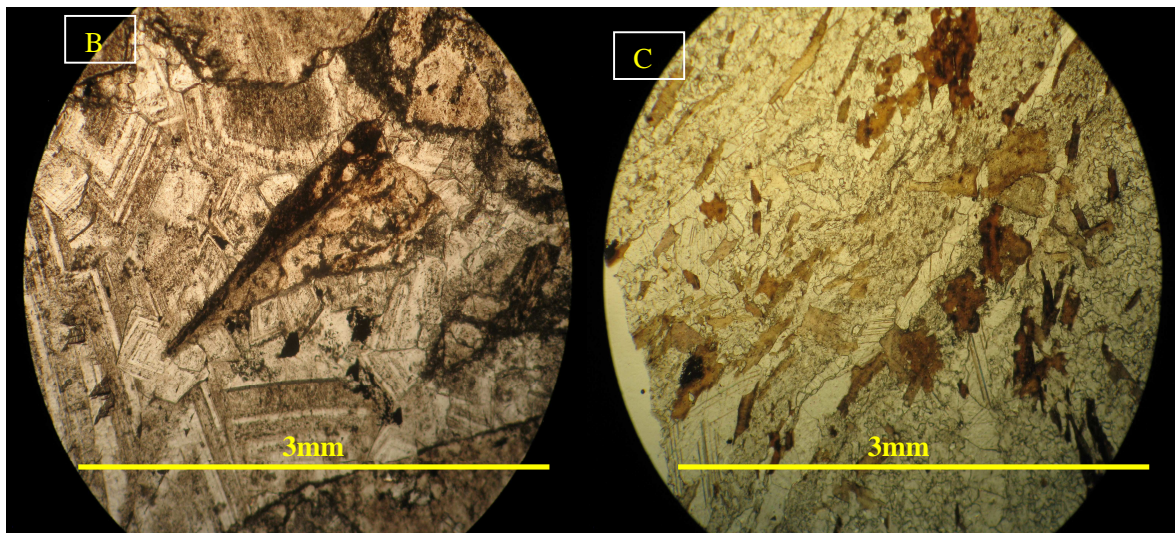


Figure. 10: B. Photomicrograph of SD782-SD29. Rhomb-shaped dolomite and calcite in a breccia. C. SD782-SD33. Biotite and calcite matrix with the biotite cross-cutting the coarse-grained calcite veins.

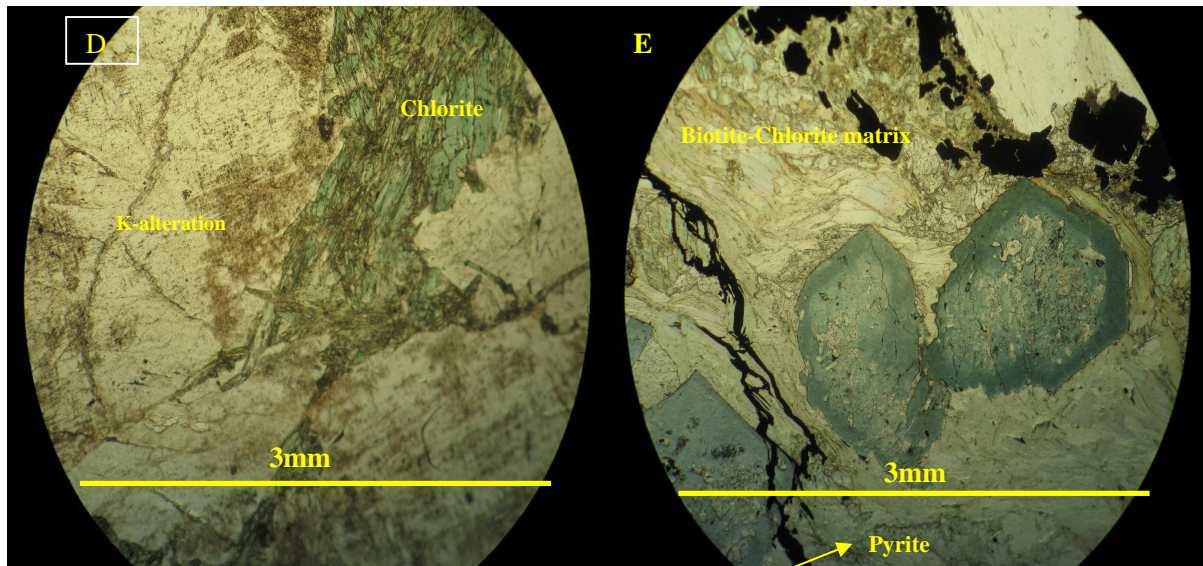


Figure. 11: Photomicrographs of D: SD129-SD77. Chlorite alteration developed in a potassic-altered sample. Less than 1% of sulphide mineralogy can be observed in this sample.

E: SD119-SD60B. Chlorite-biotite alteration developing around the zoned tourmalines crystals. Sulphide precipitation (mainly pyrite) occurs in the open spaces on the rock and the tourmaline crystals.

#### 4.5 Ore Petrography

The main sulphides in the samples include pyrite and arsenopyrite with minor pyrrhotite. The arsenopyrite crystals are euhedral. Pyrite is irregular, anhedral and exhibits a variety of textures including frambooidal, colloform, zoning, skeletal and atoll texture. The colloform pyrite is cross-cut by a later, elongated arsenopyrite crystal. It also forms as open space fill. Pyrite inclusions occur in the arsenopyrite indicating that the pyrite is early. Both the pyrite and the arsenopyrite also occur in veins. The outer margin of the arsenopyrite veins were occupied by pyrite. Pyrite also develops in the margins of a calcite-rich vein. Concentric layering and botryoidal texture were developed in the pyrite vein.

Minor gold was observed on the pyrite edges/margins with a very small percentage disseminated in the matrix, i.e. SD782-SD17A. Less than 1% of octahedral magnetite was observed. Chalcopyrite occurs as inclusions in the hematite and sphalerite indicating that the chalcopyrite is earlier. It also occurs as an open space fill between the pyrite. The following paragenetic sequence was observed for the ore mineralogy: pyrite-chalcopyrite  $\pm$  (sphalerite + hematite) – arsenopyrite. The ore minerals and the host rocks were then brecciated as shown in sample SD129-SD72C. Open space fill texture is shown in Figure 12 with Figure 13 also show brecciation.

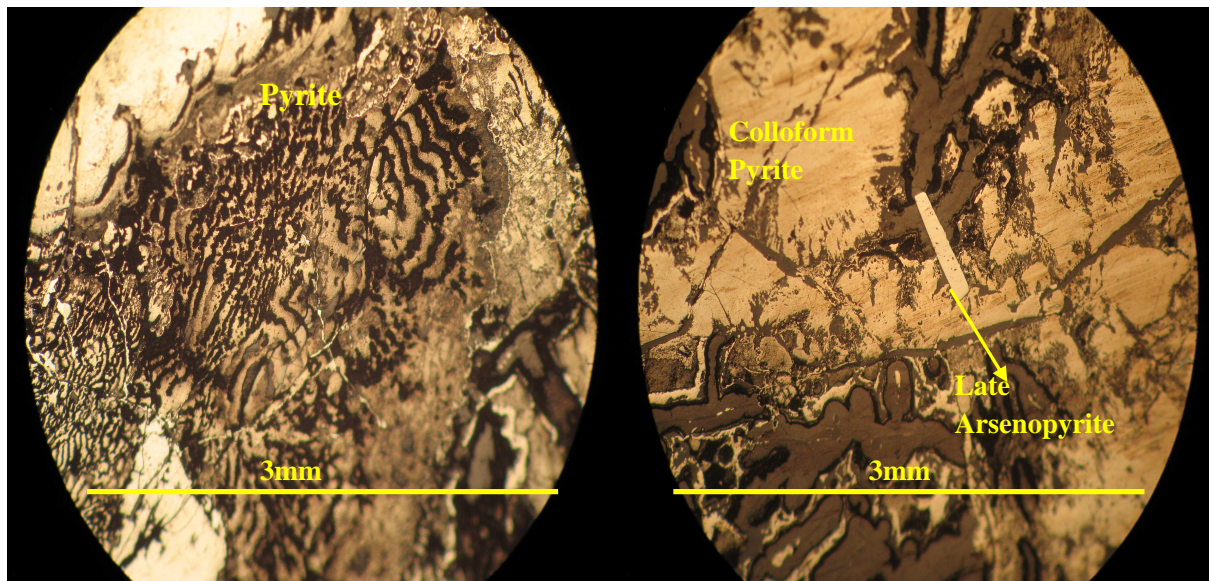


Figure. 12: Photomicrograph of Sample SD129-SD66. A: Concentric-colloform texture displayed by the pyrite. B: Colloform pyrite and the host rock (silica) being cross-cut by the elongated arsenopyrite crystals.

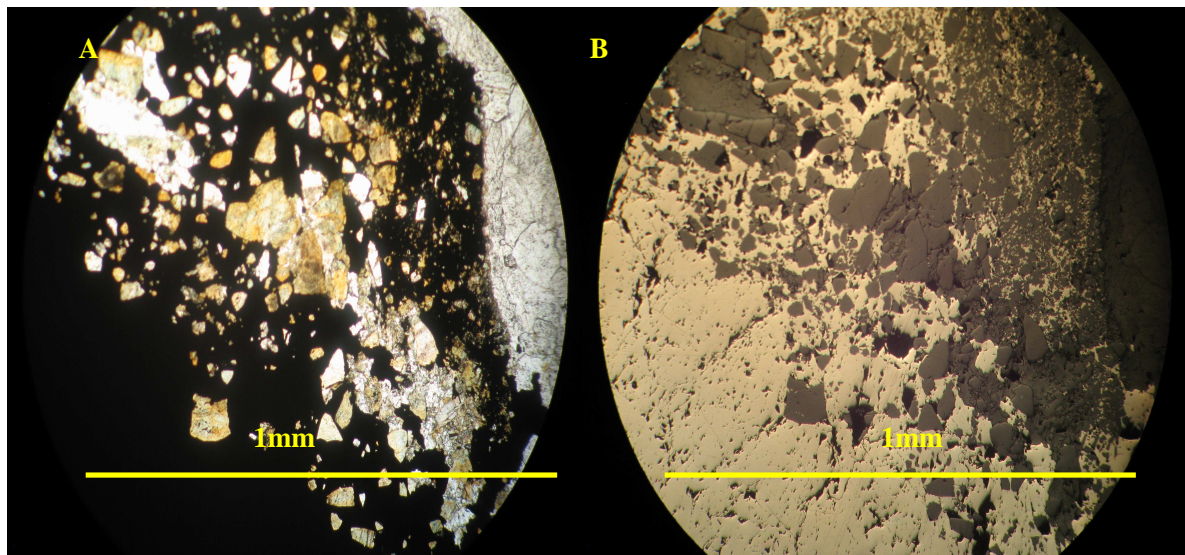


Figure. 13: Photomicrograph of Sample SD SD782-SD17A. Breccia composed of massive pyrite and biotite crystals. Taken from A: Reflected and B: Transmitted light

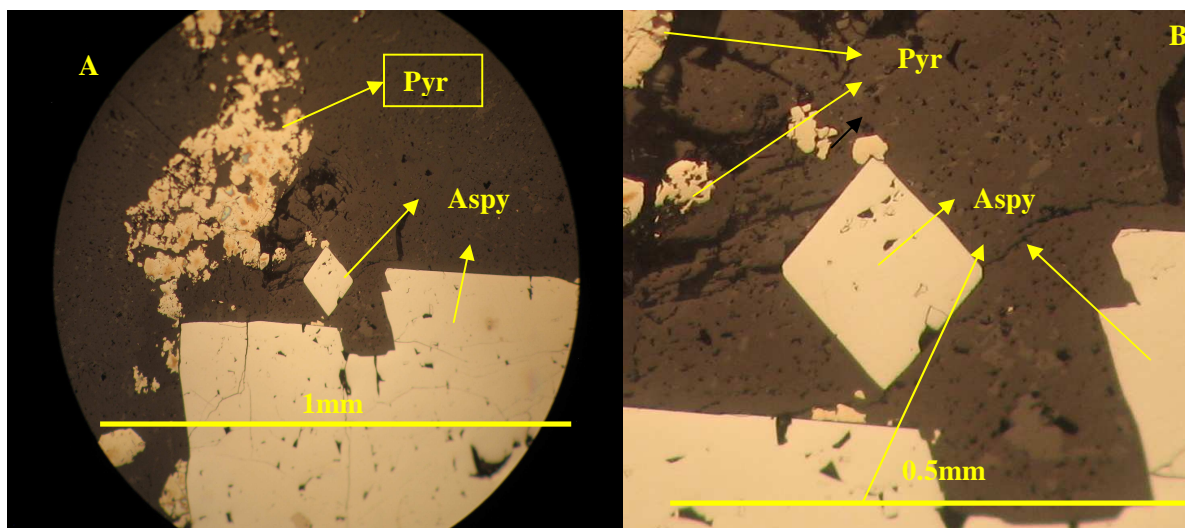


Figure. 14: Photomicrograph of Sample SD129-SD71. Euhedral arsenopyrite (Aspy) and anhedral pyrite (Pyr) which is earlier. Rhombohedral, late arsenopyrite with the pyrite in photomicrograph B.

## **CHAPTER 5: DISCUSSION**

### **5.1 Depositional Environment**

The development of seismites is interpreted as a result of either a seismic activity. These correlate with the seismites recorded by Mazumder et al (2006) which are deformations that occurred in unconsolidated sediments mainly as a result of shock. Soft sediment deformation is represented by slump facies recorded on both the Helicopter pit and the drill cores. Slumping is interpreted to have succeeded the deposition of the sediments and these occur mainly in continental slopes, seismically active environments and prior to the consolidation of sediments. The slump sequence of the main Sadiola open cast can therefore be correlated with that of the ancillary pits defined by Matabane (2008). They can also be interpreted to have formed due to overloading, rapid sedimentation, over-steepening of slopes by earthquakes (Bagati, 2008). The slumps structures are therefore interpreted to have formed in continental slope or a seismically active area before the sediments were lithified.

The sandy-metasediments and metagreywacke are deposits of fluvial to marine systems. Fluvial deposits are cross bedded, similar to the cross-bedded sandy-metasediments of the Helicopter Pit. They are also influenced by the velocity of water moving the particles. The metagreywacke are deposits of shallow marine waters. The cross-bedded sandy-metasediments corresponds to the sandstones of Martin and Turner (1998) and Tucker (2001), which are deposited on high kinetic environments including braided rivers, deltas, shallow marine and continental margins. The shallow-marine metagreywacke are interpreted by Tucker (2001) to have been deposited by turbidity currents mainly off continental margins. The turbidites were deposited as a result of turbidity currents. They greywacke observed in the field are similar to that of Dampare et al. (2004) which are fine-medium grained and show some degree of metamorphism. The Helicopter pit metasediments are also similar in that they are massive and show minimal sedimentary structures. These are therefore interpreted to have formed in an active continental margin tectonic setting (Dampare et al., 2004).

From the interpretation and the comparison made above, the Sadiola open cast lithologies are representative of continental and shelf margins. This is based on the fact that along these settings, there is sediment instability, turbidity currents, slumps and rapid sedimentation. The sandy metasediments are deposits of fluvial to shallow marine settings.

## 5.2 Structural Interpretation

The two deformation phases that are identified in the study areas of the Sadiola goldfield correlate with the deformation phases interpreted by Hein (2009) in the Goren greenstone belt in Burkina Faso, Tshibubudze et al., (2009) in the Markoye Shear Zone in Burkina Faso. The first deformation is characterized by the development of NNW-trending folds (F1). NNW bedding and cleavage (S1) orientation associated with D1 are recorded in the study area. This deformation is termed the Tangaean Event and formed during the NE-SW shortening period. Quartz veins formed during this event and their dominant trend is towards NNE-NE.

The second deformation event is characterized by the development of ENE-ESE trending folds (F2) and NE-trending cleavage (S2). The ENE trending fold axes concur with Voet's (1997). The second deformation correlates with the 2.13 - 1.98 Ga Eburnean orogeny as defined by Feybesse et al (2006). A conclusion can thus be made that the rocks of the Sadiola open cast mine underwent at least two phases of deformation.

## 5.3 Petrographic Interpretation

Majority of the recorded mineral assemblage are interpreted to have formed in conditions of contact metamorphism, hornfels facies and at low temperature settings. They are of metamorphic origin. These assemblages are of lower greenschist metamorphic facies. Brecciation occurred in the marble and is attributed to have resulted from the fluids passing through the rock. This is consistent with the interpretation of Theron's (1997a) that gold skarns develop where carbonates are present. These fluids are also responsible for the deposition of calcite and sulphide (mainly pyrite) in the open spaces. The occurrence of albite is interpreted as a result of the hydrothermal introduction of Na into the system (Theron, 1997a). The fluids at the Sadiola open cast are therefore interpreted to be hydrothermal in origin. The texture displayed by the biotite (Fig. 6) is the syntectonic deposition of biotite which is followed by an open space fill of calcite. Under conditions of contact metamorphism, there is a spatial relationship between the intrusion and the mineralisation. The mineralisation is observed in the low temperature rocks located further away from the high temperature setting closer to the intrusion.

Chlorite replaces biotite and this texture is accompanied by potassic alteration. Potassic alteration recorded consists of biotite, quartz and potassic feldspar (mainly albite). Carbonate alteration is present in the form of dolomite rather than calcite. Dolomite is recrystallising at the expense of calcite. Sulphide precipitation occurs with biotite. An increased biotite concentration occurs with higher sulphide precipitation. The occurrence of epidote and chlorite is interpreted as the alteration of hornblende. The occurrence of tourmaline is interpreted to have resulted from the infiltration of boron-rich fluids (London, 1986) while the cordierite can be as a result of high-grade hornfels metamorphism.

The vein growth that has been recorded from thin sections is crack-seal and open space fill and these are mainly quartz-carbonate and quartz-sulphide veins. An association between sulphide precipitation and biotite-chlorite alteration is observed. The veinlets are interpreted as to have formed during brittle deformation with the presence of stylolitic structures indicating dissolution. These features correlate with those of Wilson (2002b).

The radial/concentric textures observed in Figure 9 are due to physical and chemical variation in fluid chemistry. The skeletal and framboids pyrite textures are common in rapidly cooling rocks and at low temperatures. The skeletal intergrowths of pyrite are the replacements products of pyrrhotite and they are associated with retrograde replacement of amphiboles (Edwards, 1947). The ore mineral-suite for the Sadiola gold mine includes Au-As-Fe-S and minor Zn-Sb-Cu. This ore mineral suite has been recorded in the study area by Wilson (2002a). The temperature range at which the pyrite-arsenopyrite-gold mineralisation forms was recorded by Mikus and Chovan (2003) to be in a range of 385 – 465 °C, and this was in the Au-Sb mineralisation.

The biotite texture observed in figure 9 can therefore be interpreted as the biotite isograd defined by Blatt and Tracy (2006) which is represented by the equation: muscovite + quartz + ankerite = biotite + calcite + carbon dioxide. The presence of chlorite in the biotite rocks indicates that the chlorite is also as a result of the above equation.

The recorded calc-silicate and potassic alteration is similar to that of Boshoff et al, (1998) and Theron (1997a). Gold and pyrite-arsenopyrite assemblage are interpreted to have formed during the potasssic-alteration stage (Boshoff et al., 1998). This stage is also associated with the chlorite-biotite alteration during carbonate alteration. The observed skarnification in the carbonate are characterised by biotite, amphiboles, pyrite, magnetite and calcite. These are as a result of fluid flux into the carbonate system. Theron (1997a) indicated that this is due to the introduction of Si, Fe and Mg by hydrothermal fluids during contact metamorphism and the alteration development.

Gold mineralisation is interpreted to occur with chlorite-biotite alteration. This is also associated with potasssic alteration. It is relatively associated with the pyrite-arsenopyrite mineral assemblage. It is also interpreted to occur along the biotite isograd which occurs between the inner to middle contact aureoles (Hein and Tshibubudze, 2007a, b). Gold mineralisation forms along the Sadiola Fracture Zone interpreted as the carbonaceous-siltstone greywacke unit. The chlorite-biotite alteration and the breakdown of hornblende into epidote, chlorite and quartz occur along the inner-middle transition boundary. Carbonate alteration is interpreted to have formed in association with the gold forming stages.

The resulting fluid circulation, textures observed and the occurrence of the contact aureoles indicate that the Sadiola gold mine and the resulting mineralisation have a spatial and temporal relationship to

intrusions. The mineralisation at Sadiola is therefore interpreted to be as a result of metamorphism and deformation brought about the Sekokoto pluton emplacement during the Eburnean orogeny. Structural data indicate that quartz veins formed prior to the development of the S2 cleavage systems. These are therefore interpreted to be post-Tangaean and pre-Eburnean and are associated with minor pyrite-arsenopyrite mineralisation. Mineralisation was therefore upgraded by pluton emplacement and the reactivation of the Sadiola Fracture Zone and the remobilisation of fluids to cause brecciation and skarnification of the carbonate unit. The fluids have moderate to high salinity as determined by Pan and Fleet (1992) from calcite-dolomite geothermometry.

#### 5.4 Comparison to Sadiola goldfield with the rest of the West African Gold deposits

The Sadiola deposits share some similarities with the other gold deposits in the West African Craton. In the nearby FE3 open cast, two styles of gold mineralisation were recorded by Matabane (2008). These are gold mineralisation in the breccia lodes and in the upper slump facies which co-exists with arsenopyrite-pyrite assemblage and the secondary placer gold mineralisation. Similar occurrence of orogenic gold systems are recorded in Ghana, Senegal, Burkina Faso, Guinea and Cote d'Ivoire (Goldfarb et al., 2001). Primary gold deposits in Burkina Faso are classified as orogenic-type gold deposits (Béziat et al., 2008) with the differences from the Sadiola documented in the style of gold mineralisation. Two styles of mineralisation observed in Burkina Faso are quartz-vein and disseminated (Béziat et al., 2008). Disseminated sulphides gold mineralisation described by Béziat et al (2008) are interpreted to be equivalent to the sulphide-ore type of Ashanti and Chirano deposits in Ghana and Yaouré-Angovia deposits in Cote d'Ivoire. The Loulo goldfield, SSE of Sadiola, is characterised by gold mineralisation which is hosted in the Kofi Formation in tourmaline-rich quartz veins (Wilson, 2002). The Loulo deposit is associated with earlier extensional veins and occurs mainly in the Lower Birimian sequence (Fouillac et al., 1993; Béziat et al., 2008). In Ghana, gold mineralisation occurs in conglomerate beds in the Tarkwa District (Milési et al., 1992). Gold occurs also in five parallel NE-trending greenstone belts in Ghana.

## **CHAPTER 6: Conclusion**

- The mineral assemblages of the Sadiola open cast are representative of greenschist metamorphic facies.
- Sadiola lithologies underwent at least two deformation events: one associated with the Tangaean event (D1) and the latter associated with the Eburnean orogeny (D2).
- The quartz veins are interpreted to have formed in the D1 event during a NE-directed compression.
- Sadiola lithologies underwent two metamorphic events: regional metamorphism to lower greenschist facies and contact metamorphism to hornblende-hornfels facies.
- Gold mineralisation is associated with a variety of alteration system with pyrite-arsenopyrite mineral assemblage.
- Mineralisation tends to occur along the carbonate-greywacke contact which is from the inner contact aureole to the middle aureole.
- The transition from the inner to middle contact aureole is indicated by the breakdown of hornblende into chlorite, epidote and quartz and from rocks that were completely recrystallised to rocks in which the primary bedding is preserved.
- This is the Sadiola Fracture Zone which was re-activated during pluton emplacement and was used as the pathway for moderate-high salinity fluids.
- The Sadiola open cast mine is interpreted as an Intrusion related gold deposit or a thermal aureole gold deposits associated with the Sekokoto plutons.

## **References:**

- Béziat, D., Bourges, F., Debat, P., Lompo, M., Martin, F., Tollon, F., 2000. A Palaeoproterozoic ultramafic-mafic assemblage and associated volcanic rocks of the Boromo greenstone belt: fractionates originating from island arc volcanic arc in the West African craton. *Precambrian Research*, 101, 25-47.
- Blatt, H., Tracy, R.J., Owens, B.E., 2006. *Petrology: Igneous, Sedimentary and Metamorphic*, 3<sup>rd</sup> Edition, W.H. Freeman and Company, New York, 530p.
- Boshoff, F., Hanssen, E., Hill, J.V., Jones, D., Kaisin J., Traore, S., Voet, H.W., 1998. The Sadiola Hill Mine: A lower Proterozoic gold deposit in the Kéniéba window-Mali, West Africa. Unpublished report to Anglo American, 6p.
- Craig, J.R., and Vaughan, J.D., 1981. *Ore Microscopy and ore petrography*. John Wiley & Sons, Inc, Canada, 406p.
- Dia, A., Van Schmus, W.R., Kroner, A., 1997. Isotopic constraints on the age and formation of a Palaeoproterozoic volcanic arc complex in the Kedougou Inlier, eastern Senegal, West Africa. *Journal of African Earth Sciences*, 24, 197-213.
- Dioh, E., Béziat, D., Debat, P., Grégoire, M., Ngom, P.M., 2006. Diversity of the Palaeoproterozoic granitoids of the Kedougou Inlier (eastern Senegal): Petrographical and geochemical constraints. *Journal of African Earth Sciences*, 44, 351-371.
- Edwards, A.B., 1947. *Textures of the ore minerals and their significance*. Australian Institute of Mining and Metallurgy, Inc, Melbourne, 185p.
- Feybesse, J., Billa, M., Guerrot, C., Duguey, E., Lescuyer, J., Milesi, J., Bouchot, V., 2006. The Palaeoproterozoic Ghanaian province, Geodynamic model and ore controls, including regional stress modeling. *Precambrian Research*, 149, 149 – 196.
- Fouillac, A. M., Domanget, A., Milési, J.P., 1993. A carbon, oxygen, hydrogen and sulfur isotopic study of the gold mineralisation at Loulo, Mali. *Chemical Geology*, 106, 47-62.
- Goldfarb, R.J., Groves, D.I., Gardoll, S., 2001. Orogenic gold and geologic time: a global synthesis. *Ore Geology Reviews* 18, 1-75.

- Groves, D.I., Goldfarb, R.J., Gebre-Mariam, M., Hagemann, S.G., Robert, F., 1998. Orogenic gold deposits: A proposed classification in the context of their crustal distribution and relationship to other gold deposit types. *Ore Geology Reviews* 13, 7-27.
- Gueye, M., Siegesmund, S., Wemmer, K., Pawlig, S., Drobe, M., Nolte, N., Layer, P., 2007. New evidence for an early Biriman evolution in the West African Craton: An example from the Kedougou-Kénéiba Inlier, southeast Senegal. *South African Journal of Geology* 110, 511-534.
- Gueye, M., Ngom, P.M., Diéne, M., Thiam, Y., Siegesmund, S., Wemmer, K., Pawlig, S., 2008. Intrusive rocks and tectono-metamorphic evolution of the Mako Palaeoproterozoic belt (Eastern Senegal, West Africa). *Journal of African Earth Science* 50, 88-110.
- Hanssen, E., Kaisin, J., Mounkoro, B., Hill, J., 1998. Sadiola deep sulphide project, Part I : Text. Unpublished company reports to IAMGOLD Corporation on behalf of SEMOS, 86p.
- Hastings, D., 1982. On the tectonics and metallogenesis of West Africa: A model incorporating new geophysical data. *Geoexploration*, 20, 295-327.
- Hein, K.A.A., 2003. The Batman and Quigleys gold deposit of the Mt. Todd (Yimuyn Manjerr) Mine, Australia: structural, petrographical and mineralogical investigations of coeval quartz sulphide vein and lode/stockwork systems. *Ore Geology Reviews* 23, 3-33.
- Hein, K.A.A., Morel, V., Kagoné, O., Kiemde, F., Mayes, K., 2004. Birimian lithological succession and structural evolution in the Goren segment of the Boromo-Goren Greenstone Belt, Burkina Faso. *Journal of African Earth Sciences*, 39, 1-23.
- Hein, K.A.A., Zaw, K., Mernagh, T.P., 2006. Linking mineral and fluid inclusion paragenetic studies: The Batman deposit, Mt. Todd (Yimuyn Manjerr) goldfield, Australia. *Ore Geology Reviews* 28, 180-200.
- Hein, A.A. and Tshibubudze, A., 2007a. Sadiola Ore Genesis Model, Sadiola Mine and satellites pits, Mali. Unpublished summary report to Société d'Exploitation des Mines d'Or de Sadiola S.A., 8p.
- Hein, A.A. and Tshibubudze, A., 2007b. Sadiola Ore Genesis Model, Sadiola Mine and satellites pits, Mali. Unpublished summary report to Société d'Exploitation des Mines d'Or de Sadiola S.A., 15p.

Hein, K.A.A., in press. Succesion of structural events in the Goren greenstone belt (Burkina Faso) : Implications for West African tectonics. *Journal of African Earth Science*.

Hein, K.A.A., 2009. High-level summary report, Research at Sadiola by the University of the Witwatersrand, Confidential Report to Société d'Exploitation des Mines d'Or de Sadiola S.A., 4p.

Heinrich, E. Wm., 1965. Microscopic identification of Minerals. McGraw-Hill, Inc, USA, 414p.

Hirdes, W., Davis, D.W., 2002. U-Pb Geochronology of Palaeoproterozoic rocks in the southern part of the Kedougou-Kénéiba Inlier, Senegal, West African: Evidence for diachronous accretionary development of the Eburnean Province. *Precambrian Research* 118, 83-99.

Holcombe, R.J., 2008. GEORient 9.4.0. Holcombe Coughlin & Associates, Australia.

Jordaan, M.J., (Comp), Traoré, S., Williams, T.P., 1994. Geological interpretation of Sadiola Hill as a guide to ore evaluation, mining and exploration. Anmercosa Exploration internal report to Société d'Exploitation des Mines d'Or de Sadiola S.A., 27p.

Lang, J.R., and Baker, T., 2001. Intrusion related gold system : the present level of understanding. *Mineralium Deposita*, 36, 477-489.

Ledru, P., Pons, J., Milesi, J.P., Feybesse, J.L., Johan, V., 1991. Transcurrent tectonics and polycyclic evolution in the Lower Proterozoic of Senegal-Mali. *Precambrian Research*, 50, 337-354.

Liégeois, J.P., Claessens, W., Camara, D., Klerkx, J., 1991. Short-lived Eburnian orogeny in southern Mali, Geology, tectonics, U-Pb and Rb-Sr geochronology. *Precambrian Research*, 50, 111-136.

Martin, C.A.L., and Turner, B.R., 1998. Origins of massive-type sandstones in braided river systems. *Earth Science Reviews*, 44, 15-38.

Matabane, M., 2008. The geology of the FE3 open cast, Sadiola, Mali: Stratigraphy, structure and intrusive rocks. Honours thesis, University of the Witwatersrand, Johannesburg, 56p.

Matabane, M. and Hein, M.R., submitted. Stratigraphy of the Kofi Series in the FE3 Open-Casts, Sadiola Goldfield, Kedougou-Kénéiba Inlier Mali. *Journal of African Earth Sciences*.

Mazumder, R., Van Loon, A.J., Arima, M., 2006. Soft sediment deformation structures in the Earth's oldest seismites. *Sedimentary Geology*, 186, 19-26.

- Milesi, J.P., Ledru, P., Ankrah, P., Johan, V., Marcoux, E., 1992. The metallogenic relationship between the Birimian and Tarkwaian gold deposits in Ghana. *Mineralium Deposita*, 26, 228-238.
- Milesi, J., Ledru, P., Feybesse, J., Dommange, A., Marcoux, E., 1992. Early Proterozoic ore deposits and tectonics of the Birimian orogenic belt, West Africa. *Precambrian Research*, 58, 305-344.
- Peters, G.S., 2004. Syn-deformational features of Carlin-type deposits, *Journal of Structural Geology* 26, 1007-1023
- Potrel, A., Peucat, J.J., Fanning, C.M., 1998. Archean crustal evolution of the West African Craton: example of the Amsaga Area, (Reguibat Rise). U-Pb and Sm-Nd evidence for crustal growth and recycling. *Precambrian Research*, 90, 107-117.
- Ranson, R.L., 1998. Structural modelling of the Sadiola Hill Gold Deposit, Mali, MSc thesis, University of Exeter, England, 104p.
- Sheets, R., and Moore, J., 2000a. Annual review: Sadiola deep sulphide drilling project, unpublished report to the Chief geologists, Sadiola Hill Mine, Mali, Rhodes University, Grahamstown, 6p.
- Sheets, R., and Moore, J., 2000b. Preliminary stable isotope geochemistry for deep sulphide zone, Sadiola Hill Deposit, Mali: Implications for using stable isotopes in exploration, unpublished report to Sadiola Hill Mine, Mali, Rhodes University, Grahamstown, 26p.
- Stephens, J.R., Mair, J.L., Oliver, N.H.S., Hart, C.J.R., Baker, T., 2004. Structural and mechanical controls on intrusion-related deposits of the Tombstones Gold Belt, Yukon, Canada, with comparisons to other vein-hosted ore deposit types. *Journal of Structural Geology* 26, 1025-1041.
- Theron, S.J., 1997. The intrusive and extrusive rocks from the Sadiola concession area: A petrographical and geochemical study, 6 February 1997. Unpublished AARL and Base Metal Unit Report No. M96X5071, 50p.
- Theron, S.J., 1997a. Possible genetic model for gold mineralization within the greater Sadiola concession area. Unpublished report to IAMGOLD/AGEM, 3p.
- Thompson, J.H.F., Sillitoe, R.H., Baker, T., Lang, J.R., Mortensen, J.K., 1999. Intrusion-related gold deposits associated with tungsten-tin provinces. *Mineralium Deposita* 34, 323-334.
- Tshibubudze, A., et al. The Markoye Shear Zone in NE Burkina Faso. *J. Afr. Earth Sci.* (2009), doi:10.1016/j.jafrearsci.2009.04.009

- Tucker, M., 2001. Sedimentary Petrology, 3<sup>rd</sup> Edition, Blackwell Sciences, Ltd, Oxford, 262p.
- Van der Merwe, S., 2002. The Sadiola deposit: a structural deposit of the deep sulphide mineralisation, unpublished report to Anglo American Corporation of South Africa Limited, Johannesburg, 30p.
- Voet, H.W., 1996. The Sadiola Hill orebody in western Mali- A giant diorite gold porphyry deposit with Carlin-like characteristics. Unpublished report to Anglo American Corporation of South Africa Limited, 15p.
- Voet, H.W. 1997. Cross folding at Sadiola Hill Mine and the possible extent of the orebody to the south. Unpublished report to Unpublished report to Anglo American Corporation of South Africa Limited, 3p.
- Wall, V.J., Taylor, J.R., 1991. Thermal Aureole Gold-Victoria and elsewhere, Selwyn Memorial Lecture Series, Melbourne, 4p.
- Wilson, G.C., 2002. Alteration styles and host lithologies of mineralisation at the Sadiola Gold deposit, Mali, IAMGOLD Corporation, Mali, 35p.
- Wilson, G.C., 2002a. Mineralogical and Textural descriptions of carbonate and clastic metasediments and intrusive rocks from the Sadiola Gold Deposit, Mali, IAMGOLD Corporation, Mali, 42p.
- Wilson, G.C., 2002b. Sulphides and alteration assemblages in drill core from the Sadiola Gold Deposit, IAMGOLD Corporation, Mali, 42p.
- US Department of State, 2009. Background Note, Bureau of African Affairs, July 2009.

## Appendix

### Petrography

#### SD782-SD33

Very fine-grained matrix composed of quartz, calcite, dolomite and randomly oriented biotite. Sample is layered, with the layering indicating the process of skarnification. The sample is interpreted as being from the Sadiola west wall from the bedded carbonate.

Modal abundance:      Calcite: 55%

Biotite: 30%

Quartz: 14%

Sulphides: 1%

#### SD782-SD28B

Sample contains chloritoid which is randomly oriented in a fine-grained matrix of quartz, calcite and minor biotite. The chloritoids also occurs as porphyries. The sample is compositionally layered. The chloritoids are cross-cuts by the coarser calcite vein.

#### SD782-SD29

Shows a layering texture which is comprised of calcite and dolomite (with dolomite being the substrate). The texture develops as a result of open space fill. The inner dolomites grains have sulphides minerals associated with it. Mineral growth, fluid chemistry and the sulphide precipitation can then be interpreted.. The whole sample was then brecciated and the later sulphides were precipitated.

#### SD119-SD60B

The sample consists of the following mineralogy: zoned, hexagonal tourmaline which is surrounded by biotite. The biotite has a kinked cleavage and is cross-cut by the later sulphides. Feldspar alteration is indicated by the feldspar replacing the quartz and the biotite-chlorite replacement. Dolomitisation also occurs and is common in the calcite, where the dolomite-grains still has the calcite cleavage developed in them. Fine grained matrix of quartz, biotite and chlorite.

### SD22-SD43

The sample shows multiple dolomite veins, with the dolomite grains forming a triple-point grain contact. Biotite isograd from coarse grained matrix into fine grained matrix.

Modal Abundance:      Biotite: 20%

Quartz: 15%

Dolomite: 25%

Calcite: 20%

Sulphides: 20%

### SD782-SD16

The sample is dominated by quartz, chlorite, hornblende, cordierite and biotite. Radiating biotite textures with the replacement between chlorite and biotite giving rise to chloritisation.

Modal Abundance:      Quartz: 60%

Biotite: 11%

Chlorite: 11%

Cordierite: 2%

Hornblende: 10%

### SD129-SD74A

Epidote-rich sample and the epidote grains are highly deformed. Minor quartz and interlocking calcite grains. Triple-point grain contacts with stylolitic texture developed between some of the grains. The epidote grains are highly fractured and are scattered at some locations. There are no visible biotite and sulphides in the sample.

### SD129-SD75A/75B/75C

These three thin section are all from sample SD129-SD75 and have been cut at different places. Consists of zoned, twinned chloritoid grains, with a euhedral outer shape and a semi-rounded inner shape. These can be interpreted as chloritoid overgrowths. There is a strong potassic alteration in 75A and 75C. There is no boundary between the fine grained matrix and the coarse grained matrix (just a gradational transition with a change in grain size only). The samples are comprised of quartz, minor albite, epidote and chloritoid. Sample SD75C also has calcite.

### SD129-SD77

This is a potassic-alteration rich sample. It is dominated also by chlorite, biotite mineralogy. The sample is cross-cut by a fine grained calcite-rich vein.

### SD22-SD37B

The sample is dominant in calcite mineralogy: coarser and finer calcite which is separated by the biotite. The coarser calcite is cross-cut by a quartz-rich vein, and the quartz has about 1% calcite inclusions with the biotite developing on the edges. The biotite is also kinked.

Modal Abundance:      calcite: 70%

                        Biotite: 20%

                        Quartz: 10%

### SD782-SD32B: Marble

The sample has fine-grained matrix of quartz-calcite-biotite with the biotite also as a transition from the fine-grained to the coarse-grained matrix. It also has euhedral (cubic)-elongated sulphides. Coarse grained calcite vein cross-cuts the sample. The quartz grains have undulose extinction.

Modal Abundance:      Calcite: 38%

                        Biotite: 25%

                        Quartz: 12%

                        Sulphides: 25%

## **Ore petrography**

### **SD129-SD71**

Ore mineralogy: disseminated frambooidal pyrite

Euhedral, rhombs of arsenopyrite

Disseminated chalcopyrite

The chalcopyrite is the later sulphide. Later arsenopyrite enclosing the earlier pyrite and chalcopyrite. The paragenesis is as follows: pyrite-chalcopyrite-arsenopyrite.

### **SD129-SD66**

Ore mineralogy: pyrite

Later elongated rhombs of arsenopyrite cross-cutting the pyrite and the host rock.

Chalcopyrite

The sample shows a zoning texture in both the sulphides and the host rock. The pyrite also shows a colloform texture. The pyrite in this sample shows the following texture: zoning, colloform and curved laths of herring-bone texture.

### **SD119-SD60B**

Ore mineralogy: pyrite

The pyrite forms in open space between the host rocks lithologies.

### **SD22-SD43**

Ore mineralogy: hematite

Sphalerite with inclusions of chalcopyrite

Subhedral to euhedral pyrite

All these minerals are disseminated in the sample. The following paragenesis is then proposed: pyrite-chalcopyrite-sphalerite

## Core Logging Results

**SD022:**

Depth (m)	Lithologies	Alteration	Mineralogy	Comments
277.63			Quartz Minor Sulphides Hornblende Hornfels Chloritoid	Zoned Vein: Outer margin of sulphides and inner quartz-rich margin  The hornblend and chloritoid spots are randomly oriented  The unit is fractured and lead to silica deposition
336.00			Sulphides (pyrite) Calcite	Mineralised mottled greywacke  Part of the transitional boundary
339.0		Mineralised Zone Intense Sulphidation Calc-silicate	Sulphides (pyrite, pyrrhotite) Epidote Phlogopite Calcite spots	Starts off with greywacke- sulphide rich and grading into inner sulphides-rich then into sulphide-carbonate- rich.  Multiple fracturing system, silica vein development  Oxidised zone yielding very bright pyrites  The zone is friable
337.0				
415		Silicification Slumping	Calcite Quartz Muscovite Minor Epidote	Primary bedding preserved  Mud-rich and Carbonate-rich layers

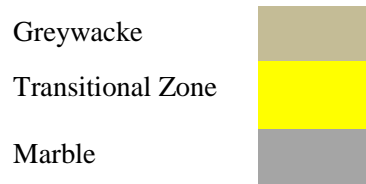
Hole Size : 0-20m HQ  
29-508m : NQ  
Azimuth : 100°, Dip : 60°

Legend  
Greywacke  
Marble  
Transitional Zone

**SD048**

Depth (m)	Lithologies	Alteration	Mineralogy	Comments
89.7			Epidote Hornblend Hornfels Chloritoid spots	Fractured unit with silica development
174- 175		Mineralised Zone Intense Sulphidation Silicification	Sulphides (pyrite, pyrrhotite) Epidote Quartz Calcite	Slumping Primary bedding destroyed Mixed Zone
219.5		Silicification Slumping K-alteration	Calcite Quartz Ankerite	Primary bedding preserved Stylolites developed at about 194m

Legend



**SD042**

Depth (m)	Lithologies	Alteration	Mineralogy	Comments
90.0		Minor K-alteration Silicification Sulphidation	K-altered calcite spots Pyrite Chloritoid spots Hornblend	The chloritoid spots are randomly oriented K-alteration becomes richer down core Pyrite develops around the euhedral quartz in calcite vein and in open spaces
200.6		Mineralised Zone Intense K-alteration Calc-silicate Silicification	Sulphides (pyrite, pyrrhotite) Epidote Phlogopite Calcite spots	Starts off with greywacke- sulphide rich and grading into inner sulphides-rich then into sulphide-carbonate- rich. The unit is friable down core Skarnification The zone is strongly altered
233-234		Silicification Slumping K-alteration around the veins	Calcite Pyrite	Euhedral quartz in a calcite vein Mud-carbonate layers Drag Folds → ↗
267.2				

Azimuth : 90°, Dip : 60°

Elevation 125m

**SD119**

Depth (m)	Lithologies	Alteration	Mineralogy	Comments
121.0		K-alteration intense up-core  Calc-silicate  Silicification	Quartz  Minor calcite  Hornblende- Hornfels spots  Quartz veins  Disseminated pyrite  Pyrrhotite in a vein  Tabular-Flaky Biotite  Chloritoid	Sulphide precipitation is in a vein  Tabular to spotted Biotite-Hornblend- Hornfels which are randomly oriented  Medium-Coarse grained
246.7		Mineralised Zone  Minor K- alteration  Slumping	Quartz  Biotite  Calcite  Ankerite	Brecciated  Carbonate dominant down core
325.0		Silicification  Slumping  K-alteration	Calcite  Quartz  Tabular Biotite  Ankerite	Grades from marble to medium-coarse grained slumped carbonates then into marble again.
501				

46

Hole Size : 0-120m RC

120-501m : NQ

Greywacke



Transitional  
Zone



Marble

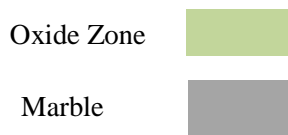


Azimuth : 100°, Dip : 55°

**SD782**

Depth (m)	Lithologies	Alteration	Mineralogy	Comments
93.0		Fe-alteration Metasediments Sandy-silty texture Slump facies	Fe-alteration	Oxide Zone
183.5			Quartz Biotite Calcite Ankerite	Slumped Brecciated Pure Carbonate unit
325.0				
501		Silicification	Calcite Quartz Biotite Ankerite	Marble unit with varying textures.

Legend



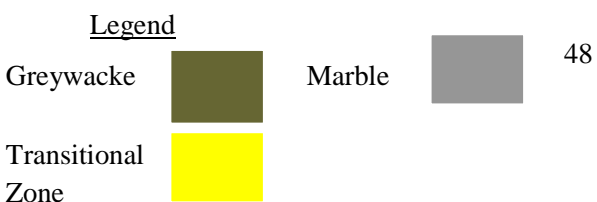
**SD129**

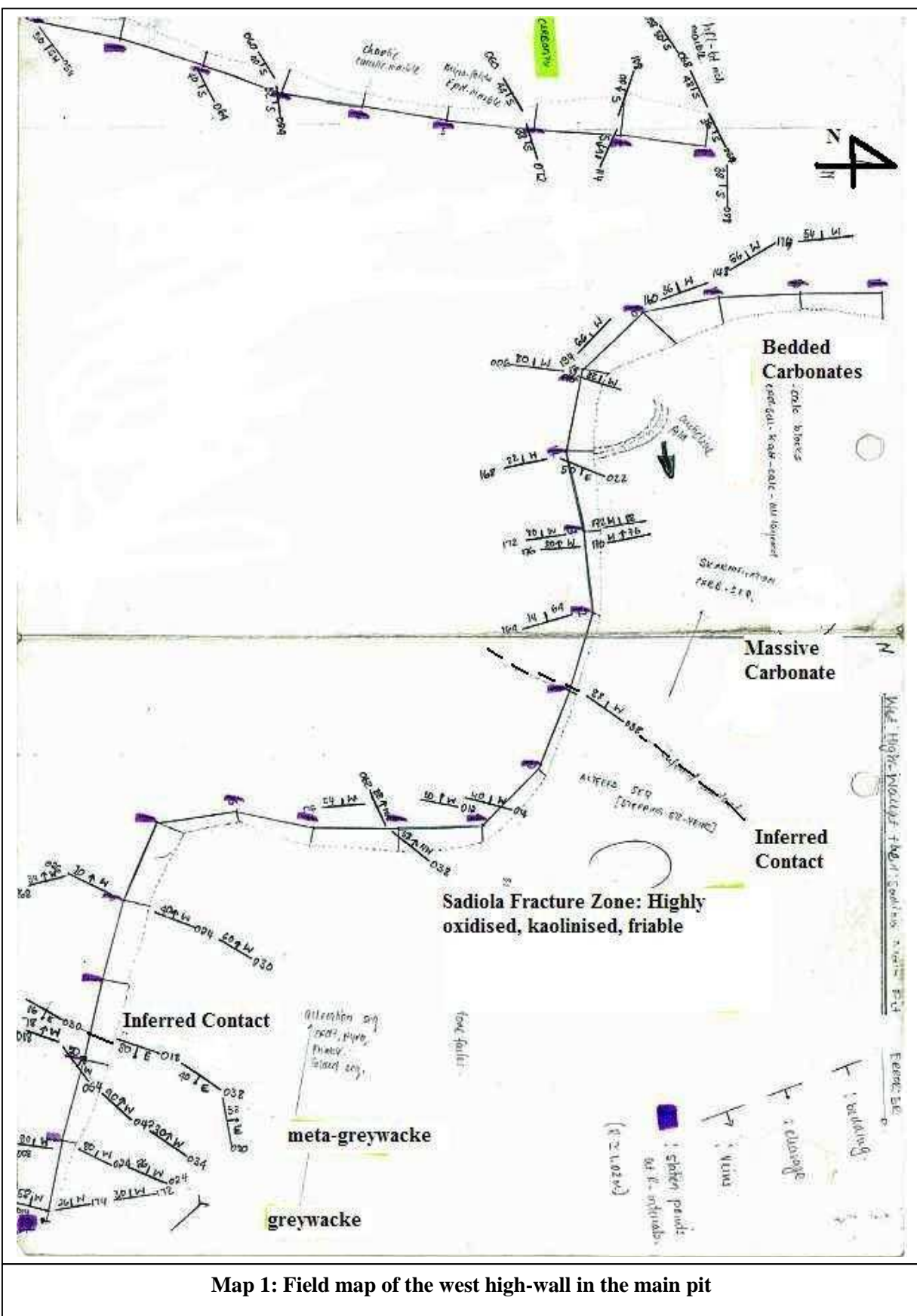
Depth (m)	Lithologies	Alteration	Mineralogy	Comments
91.0		Intense Calc-silicate & K-alteration  Minor Silicification	Quartz veins  Disseminated pyrite  Pyrrhotite in a vein  Tabular to elongated Biotite, Hornblende Chloritoid spots	Varies from sandy to quartz composition  Zoned veining (quartz-calcite veins with pyrite and pyrrhotite)  Coarse grained  Equigranular texture  Euhedral hornblende crystals
318.0		Mineralised Zone  Minor K-alteration  Silicification	Quartz  Pyrite and pyrrhotite	Grading from greywacke to marble
344.0		Silicification  Slumping  K-alteration	Calcite  Quartz  Tabular Biotite  Ankerite	Grades from marble to medium-coarse grained slumped carbonates then into marble again.
501				

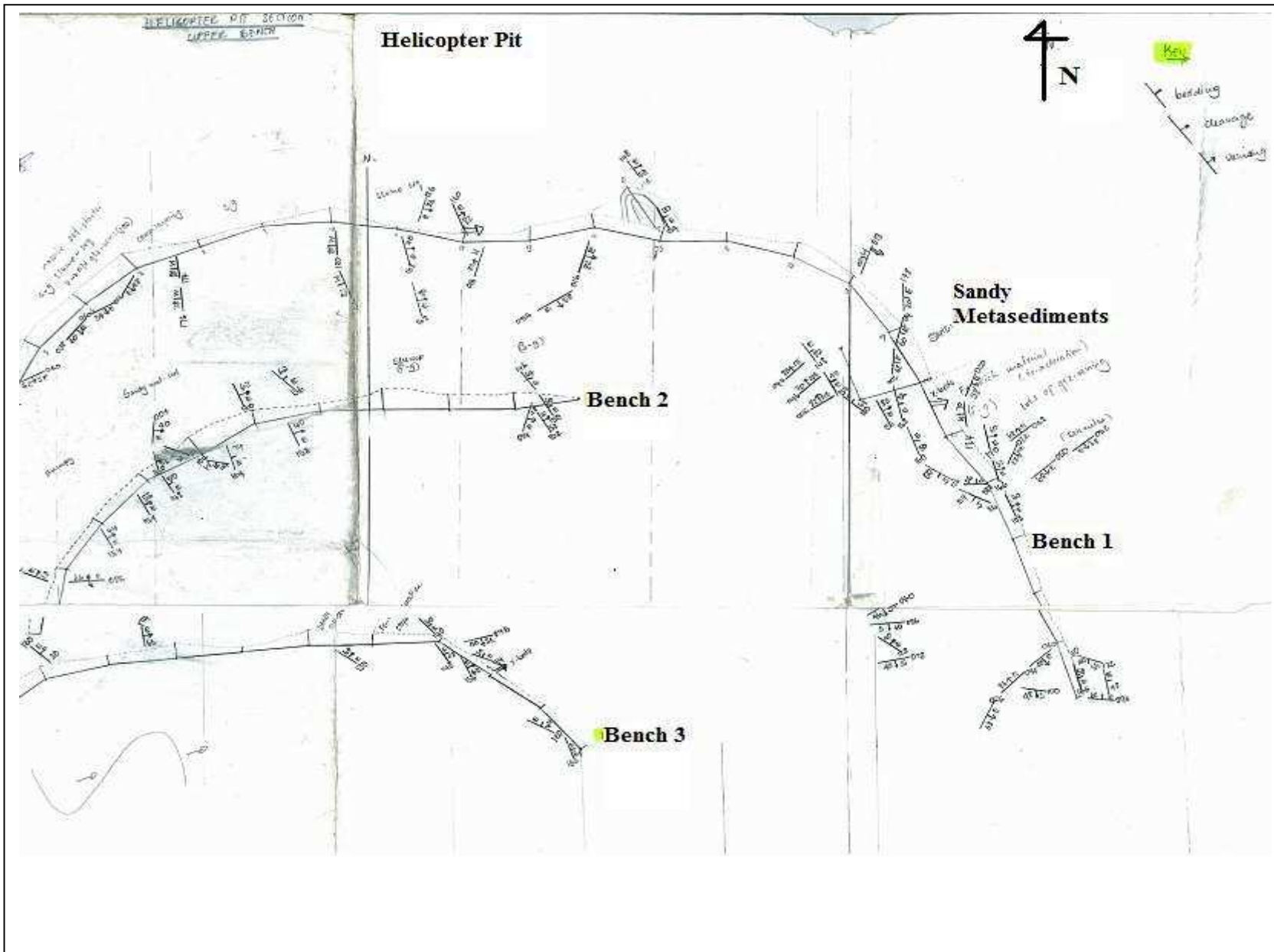
Hole Size : 0-90m RC

90-501m : NQ

Azimuth :  $100^{\circ}$ , Dip :  $55^{\circ}$







50

**Map 2: Field Map of the Helicopter Pit**